

**ANALYTIC ELEMENTS OF
ARBITRARY SHAPE**

A THESIS SUBMITTED TO THE FACULTY OF
THE GRADUATE SCHOOL OF THE UNIVERSITY
OF MINNESOTA BY

PATRICK RICHARD NEVISON

IN PARTIAL FULFILMENT OF THE
REQUIREMENTS FOR THE DEGREE OF MASTER
OF SCIENCE

DR. OTTO D.L. STRACK

DECEMBER, 2012

©PATRICK RICHARD NEVISON 2012
ALL RIGHTS RESERVED

ACKNOWLEDGEMENTS

First, I would like to thank my advisor, Dr. Otto D.L. Strack, for giving me the opportunity to pursue a graduate degree, and everything he has taught me. I would also like to thank Dr. Randal Barnes for having me as a teaching assistant, and for everything I learned from him as well. I thank Simone Gbolo-Thompson and the North Star STEM Alliance for having me as a graduate assistant. Finally, I would like to thank Bonnie Ausk, Bill Olsen, Dr. Philippe Le Grand and every one else who gave me feedback during the groundwater seminars. All of your assistance was greatly appreciated.

DEDICATION

This thesis is dedicated to my family for all of their support over the years.

ABSTRACT

The analytic element method currently uses points, lines, polygons, circles, ellipses, and curvilinear line elements to represent features in models. A new set of elements with shapes that are more general than the ellipse have been created. The elements shape is that of an equipotential around a two-legged slot. Conformal mapping was used to map the boundary of the element onto the unit circle where groundwater flow problems were solved. The inverse mapping was performed by representing the mapping function with a set of series expansions and inverting the series. Models of multiple arbitrary shaped lakes have been created. Additional shapes to represent other features such as impermeable boundaries have also been created. These new shapes allow the modeling of features that are not circular or elliptical, and can represent shapes created using a set of curvilinear line elements, with a single element.

CONTENTS

LIST OF TABLES	vi
LIST OF FIGURES	vii
1 INTRODUCTION	1
1.1 Basic Overview of Groundwater Mechanics	5
1.2 An Elliptical Lake	8
2 MAPPING THE UPPER HALF PLANE ONTO THE EXTE- RIOR OF A TWO-LEGGED SLOT	12
3 MAPPING THE ELEMENT ONTO THE UNIT CIRCLE IN THE χ PLANE	17
4 SERIES EXPANSIONS	23
4.1 Far Field Expansion	28
4.2 Expansions About the Endpoints	31
4.3 The Expansion About Corner Point One	37
4.4 The Expansion About Corner Point Two	41
5 SERIES REVERSION	46
6 ANALYTIC CONTINUATION	50
7 THE FUNCTIONS $\chi(z)$	52
8 ANALYTIC ELEMENTS	58
9 ADDITIONAL SHAPES	64
10 REFERENCES	69

A VARIOUS SHAPES	71
B BRANCH CUTS	76
C THE ANALOGOUS COMPLEX POTENTIAL	78

LIST OF TABLES

Table A.1: Two legged slots with contours of $\nu = 0.5, 0.7, 0.9$ using various values of ξ_1 and α_1 with $\alpha_0 = 0$ and $ \frac{A}{r} = 1$	71
Table A.2: Two legged slots with contours of $\nu = 0.5, 0.7, 0.9$ using various values of ξ_1 and α_1 with $\alpha_0 = 0$ and $ \frac{A}{r} = 1$	72
Table A.3: Two legged slots with contours of $\nu = 0.5, 0.7, 0.9$ using various values of ξ_1 and α_1 with $\alpha_0 = 0$ and $ \frac{A}{r} = 1$	74
Table A.4: Two legged slots with contours of $\nu = 0.5, 0.7, 0.9$ using various values of ξ_1 and α_1 with $\alpha_0 = 0$ and $ \frac{A}{r} = 1$	75

LIST OF FIGURES

Figure 1.1: Lake Calhoun fitted with an arbitrary shaped element.....	3
Figure 1.1.1: Definition of the head ϕ	5
Figure 1.2.1: The Ellipse in the z and Z planes.....	8
Figure 1.2.2: The Ellipse in the Z and χ planes.....	9
Figure 1.2.3: An elliptical lake and a well.....	11
Figure 2.1: The slot in global (a) and local (b) coordinates.....	12
Figure 2.2: The slot in the Z plane (a) and the upper half plane ζ (b).....	13
Figure 2.3: dZ (a) and $d\zeta$ (b).....	15
Figure 3.1: Equipotentials in the z plane (a) and the upper half plane (b)....	17
Figure 3.2: The upper half plane (a) and the χ plane (b).....	19
Figure 3.3: Equipotentials in the z plane (a) and in the χ plane (b) with corresponding circle of radius ν	21
Figure 3.4: A two-legged slot with contours of equipotentials with corresponding values of ν from 0.3-0.9.....	22
Figure 4.1: Domain of the far field expansion, out side the dashed line.....	25
Figure 4.2: Domains for the endpoint expansions, inside the dashed lines.....	25
Figure 4.3: The domain for the corner point expansions, inside the dashed arcs.....	26
Figure 4.4: The ring between the corner point expansions and the far field (shaded) along with the sub domains for each expansion.....	26
Figure 4.1.1: Domain of the far field expansion, out side the dashed line.....	28
Figure 4.1.2: An element (a) and an element with an improper branch cut (b).....	30
Figure 4.2.1: Domains for the endpoint expansions, inside the dashed lines..	31
Figure 4.3.1: The domain for the corner point one expansion, inside the dashed arc.....	37

Figure 4.4.1: The domain for the corner point two expansion, inside the dashed arc.....	41
Figure 6.1: The two legged slot in the z plane, along with domains for each expansion. The shaded area is to be continued into.....	50
Figure 8.1: Flownet for lakes in a field of uniform flow.....	63
Figure 9.1: The slot in the Z plane (a) and the upper half plane ζ (b).....	65
Figure 9.2: Flownet for a lake and a well in a field of uniform flow.....	66
Figure 9.3: Flownet for an impermeable object and a well in a field of uniform flow.....	67
Figure A.1: The slot in the Z plane (a) and the upper half plane ζ (b).....	73
Figure B.1: The amount the branch cuts need to be rotated about the endpoints and the adjustment for a corner point.....	76
Figure C.1: The analogous complex potential in the Z plane.....	78
Figure C.2: The analogous complex potential in the ζ plane.....	79
Figure C.3: The analogous complex potential in the χ plane.....	80

1 INTRODUCTION

The analytic element method was developed by Dr. Otto D.L. Strack of the University of Minnesota, and consists of the superposition of analytic functions to represent features in models [Strack(1989), Strack and Haitjema(1981(a) and (b))]. The analytic element method may be used in hydrogeologic settings and used to model groundwater flow. Features may be represented with points, lines, curves and closed boundaries. For closed boundaries, an ellipse for example, conformal mapping is used to map the boundary of the element onto the unit circle where the problem is solved.

The mapping for an ellipse is very similar to the Joukowski transformation created by Nikolai Zhukovskii (Joukowski), [Olver (2012)]. The mapping has more flexibility than that of the ellipse and can be used to map shapes such as airfoils and closed curves with cusps onto the unit circle. The transformation and its inverse are in explicit form, which allows direct computation of points in each domain.

An approximate conformal mapping application for simple closed curves was implemented by Edlund (1991) and applied to inhomogeneities. The approximate mapping used collocation points to form a boundary to be used for the element that would be mapped onto the unit circle. A graphical procedure was then used to check a number of points along the boundary to obtain the inverse mapping.

The control equation formulation for circular inhomogeneities was implemented by Salisbury (1992). This method gave better results than the control point formulation and allowed for the specific contribution of every other element on the inhomogeneity. This method will be used when creating analytic elements of arbitrary shape.

Solutions for two-dimensional flow through large numbers of circular inhomogeneities (e.g. 10,000) was developed by Barnes and Jankovic (1999). Each inhomogeneity was represented with a series that satisfies the Laplace equation exactly and an iterative least squares approach was used in solving for the coefficients, allowing for the precision of the solution to only be limited by the machine performing the computation. High order line elements for modeling two-dimensional groundwater flow were also developed by Barnes and Jankovic (1999).

Solutions for steady two-dimensional groundwater flow through many elliptical inhomogeneities were created by Sribhadla, Bakker, Bandilla, and Janković in 2004. The solution originated from Strack (1989) and was applied to a much larger number of elements.

In this thesis, new elements have been created to be used with the analytic element method. The new elements have a shape similar to that of an ellipse, but with more freedom. The shape can be adjusted to fit the feature that is to be represented more accurately. An example of a possible shape designed to represent Lake Calhoun in Minneapolis, MN (Google Maps), is shown in figure 1.1.

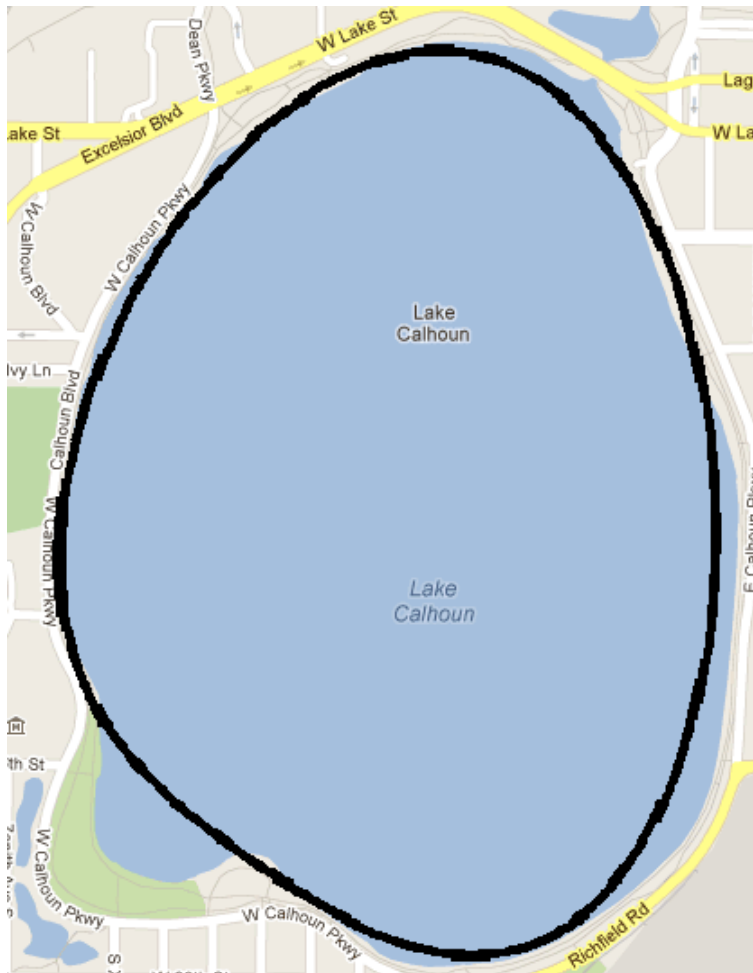


Figure 1.1: Lake Calhoun fitted with an arbitrary shaped element.

Until now, the shape of a lake would have to be represented using either a circle, ellipse or a set of curvilinear line elements. The shape chosen to represent the lake in figure 1.1 more closely matches the perimeter of a lake than would be possible with a circle or ellipse. The shape could be created by stringing together curvilinear line elements, however this can be done with a single arbitrary shaped element. The following sections will give a brief overview of groundwater mechanics and detail the construction of the new elements. Solutions will then be created for multiple arbitrary shaped lakes.

We will begin with an example of the ellipse. The ellipse is very similar in nature to the arbitrary shaped element, and will serve as in aid in understanding the general concept of constructing the solution. We will use conformal mapping to map the boundary of an ellipse onto the unit circle, and then apply the solution for a cylindrical lake.

A process similar to that of the ellipse will be used for mapping the boundary of the more general shape onto the unit circle. The more general, or arbitrary, shaped elements will take the form of an equipotential around a two-legged slot. Multiple transformations will be used to map the boundary of the shape onto the unit circle. The inverse transformation will be performed by representing the mapping functions with series expansions and inverting the series. With the transformations from the arbitrary shape to the unit circle, and from the unit circle to the boundary of the shape, we will be able to apply the solution for a cylindrical lake.

1.1 Basic Overview of Groundwater Mechanics

Groundwater flow is driven by differences in hydraulic head. The hydraulic head, $\phi[m]$ is a function of pressure, $p[N/m^2]$, the density of water, $\rho[kg/m^3]$, and gravity, $g[m/s^2]$, plus the elevation head, $h_e[m]$, which is measured from a reference level. Equation (1.1.1) is used to find the relationship between hydraulic head, pressure head and elevation head.

$$\phi = \frac{p}{\rho g} + h_e \quad (1.1.1)$$

The hydraulic head, which will be referred to as *the head*, may be found by measuring the level water rises in a stand pipe as illustrated in figure 1.1.1.

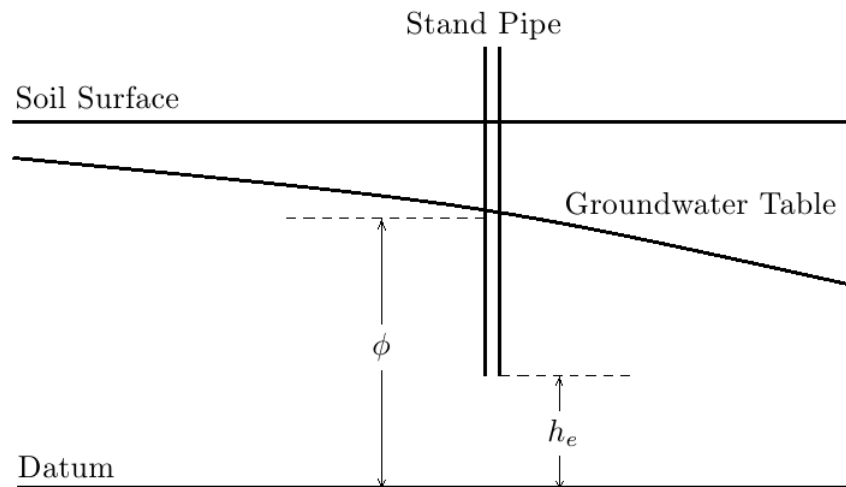


Figure 1.1.1: Definition of the head ϕ .

We will consider cases of flow in an aquifer with an impermeable base. If there is flow between two impermeable layers the flow is considered confined. If there is no upper impermeable layer, or if the elevation of the groundwater table

is below height of the upper layer, the flow is unconfined. Given the head ϕ , the hydraulic conductivity of the soil, $k[m/s]$, and the thickness of the aquifer $H[m]$, the discharge potential, $\Phi [m^3/s]$, for the case of confined flow is

$$\Phi = kH\phi + C_c \quad (\phi \geq H) \quad (1.1.2)$$

and for the case of unconfined flow the discharge potential is

$$\Phi = \frac{1}{2}k\phi^2 + C_u \quad (\phi < H) \quad (1.1.3)$$

where C_c and C_u are arbitrary constants.

We will neglect the variation in head ϕ in the vertical direction using the Dupuit-Forchheimer assumption: the resistance to flow in the vertical direction is negligible (Strack [1984]). The head is thus constant along vertical lines through the water table. We may then focus on horizontal flow, and make use of complex variables. We will use the complex coordinate system z, \bar{z} where

$$z = x + iy \quad \bar{z} = x - iy \quad (1.1.4)$$

The horizontal components of the discharge vector may then be represented with a single complex function, which is a variation of Darcy's law.

$$W = Q_x - iQ_y = -2\frac{\partial\Phi}{\partial z} \quad (1.1.5)$$

We will focus on divergence free, irrotational flow, therefore the potential will be harmonic, and the governing partial differential equation will be the Laplace equation.

$$-2\frac{\partial W}{\partial \bar{z}} = \frac{\partial^2\Phi}{\partial x^2} + \frac{\partial^2\Phi}{\partial y^2} = 0 \quad (1.1.6)$$

We will also introduce the complex potential, Ω , which is a combination of the discharge potential, Φ , and the stream function, Ψ .

$$\Omega = \Phi + i\Psi \quad (1.1.7)$$

The gradient of the the discharge potential is orthogonal to the gradient of the stream function and satisfies the Cauchy-Riemann equations

$$\frac{\partial\Phi}{\partial z} = i\frac{\partial\Psi}{\partial z} \quad (1.1.8)$$

Lines of constant discharge potential are defined as equipotentials, and lines of constant values of the stream function are defined as stream lines. Flow nets are created by plotting contours of $\Phi = \text{constant}$ and $\Psi = \text{constant}$ and choosing $\Delta\Phi = \Delta\Psi$. This can be seen from equation (1.1.8). Examples of equipotentials, streamlines, and flow nets will be used throughout the following sections. Equipotentials will also be used as part of the mapping for the arbitrary shaped element.

1.2 An Elliptical Lake

As an introduction to conformal mapping and analytic elements we will construct the solution for an elliptical lake. The boundary condition is that the head is fixed along the perimeter of the lake; the boundary of the ellipse is an equipotential. The example will follow the solution used by Strack (1989) to the problem of an elliptical lake (equipotential) and a well. The ellipse is chosen as it is a similar case to the element that will be constructed in the next section, that can be adjusted better the shape of a lake. We will use a global complex coordinate system, z , where the the foci of of the ellipse are at z_1 and z_2 . We will map the ellipse into the dimensionless local complex coordinate system, $Z = X + iY$, where the foci are located at $Z = -1$ and $Z = 1$. The transformation is given by (1.2.1) and includes a translation, rotation and change of scale as shown in figure 1.2.1.

$$Z = \frac{z - \frac{1}{2}(z_1 + z_2)}{\frac{1}{2}(z_2 - z_1)} \quad (1.2.1)$$

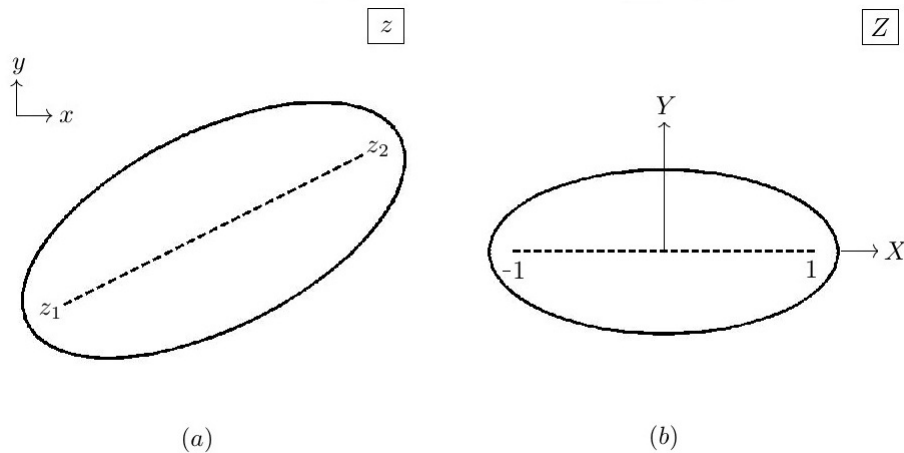


Figure 1.2.1: The Ellipse in the z and Z planes.

We will now map the unit circle in the χ plane onto the ellipse, shown in figure 1.2.2. We choose the unit circle so that we can apply the solution for a circular lake which is known, Strack (1989). One parameter is required for this transformation, ν , a positive real value less than one, that controls the shape of the ellipse. We label points 1-4 along the perimeter of the ellipse and unit circle, starting on the positive real axis, with the domain on the left. The exterior of the unit circle corresponds to the exterior of the ellipse. The following equation (1.2.2) is used for the transformation.

$$Z = \frac{1}{2} \left(\frac{\chi}{\nu} + \frac{\nu}{\chi} \right) \quad (1.2.2)$$

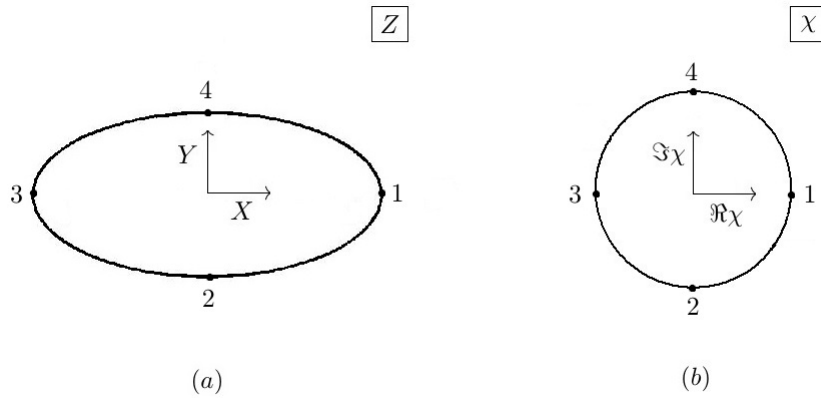


Figure 1.2.2: The Ellipse in the Z and χ planes.

We will check the boundary conditions of the transformation along the unit circle by substituting $\chi = e^{i\theta}$ into equation (1.2.2)

$$Z = \frac{1}{2} \left(\frac{1}{\nu} e^{i\theta} + \nu e^{-i\theta} \right) = \frac{1}{2} \left(\frac{1}{\nu} + \nu \right) \cos \theta + \frac{1}{2} \left(\frac{1}{\nu} - \nu \right) \sin \theta \quad (1.2.3)$$

Separating the real and imaginary parts of the function we have

$$X = \frac{1}{2} \left(\frac{1}{\nu} + \nu \right) \cos \theta \quad Y = \frac{1}{2} \left(\frac{1}{\nu} - \nu \right) \sin \theta \quad (1.2.4)$$

Using the relation $\cos^2 \theta + \sin^2 \theta = 1$ we obtain the equation for the ellipse

$$\left[\frac{X}{\frac{1}{2} \left(\frac{1}{\nu} + \nu \right)} \right]^2 + \left[\frac{Y}{\frac{1}{2} \left(\frac{1}{\nu} - \nu \right)} \right]^2 = 1 \quad (1.2.5)$$

where the denominators in each bracketed term are

$$A = \frac{1}{2} \left(\frac{1}{\nu} + \nu \right) \quad B = \frac{1}{2} \left(\frac{1}{\nu} - \nu \right) \quad (1.2.6)$$

which are the major and minor axes of the ellipse in the Z plane, respectively.

By subtracting B from A we have an expression for ν

$$\nu = A - B = A - \sqrt{A^2 - 1} \quad (1.2.7)$$

Solving for χ/ν gives two roots $Z + \sqrt{Z^2 - 1}$ and $Z - \sqrt{Z^2 - 1}$, we choose the first root because infinity in χ must correspond to infinity in Z .

$$\frac{\chi}{\nu} = Z + \sqrt{Z + 1} \sqrt{Z - 1} \quad (1.2.8)$$

We may now evaluate the complex potential for an elliptical lake and a well, Strack (1989), where χ_w is the location of the well in the χ plane, and Q its discharge there. An example of a flow net for this case may be seen in figure 1.2.3.

$$\Omega = \frac{Q}{2\pi} \ln \left[\frac{\chi - \chi_w}{\chi - 1/\bar{\chi}_w} \frac{1}{|\chi_w|} \right] \quad (1.2.9)$$

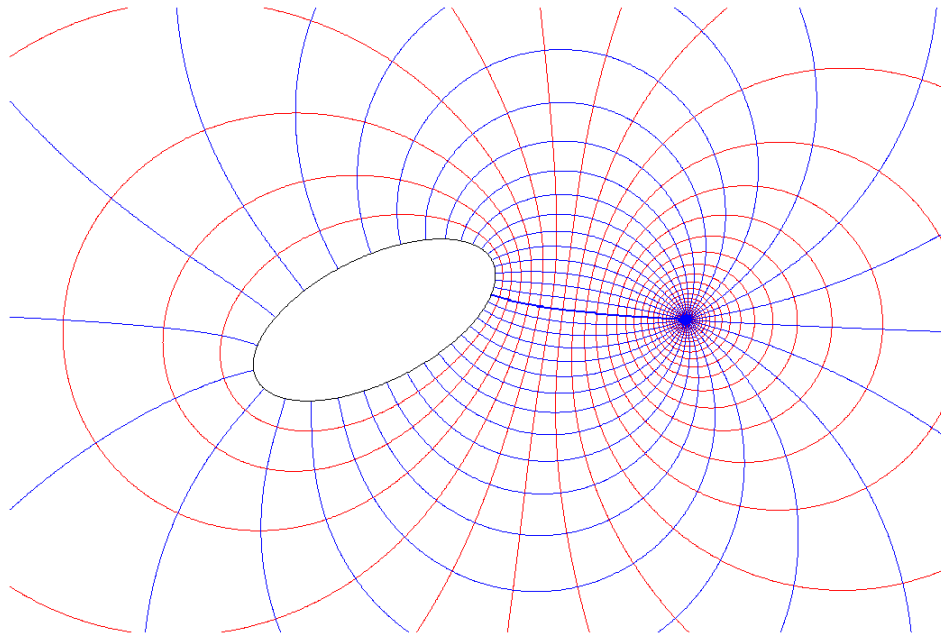


Figure 1.2.3: An elliptical lake and a well.

2 MAPPING THE UPPER HALF PLANE ONTO THE EXTERIOR OF A TWO-LEGGED SLOT

The shape of the element will be based on a two-legged slot as shown in figure 2.1. The slot has no width, and two sides. Each leg can be set at any angle and length. The slot lies in a global complex coordinate system, z , with units of length. We will make use of a dimensionless complex variable, Z , to map the slot into local coordinates. The transformation from global to local coordinates translates the intersection of the legs from the point z_0 to the origin and the size of the slot is scaled by R_1 , the length of leg that is greater than, or equal to, the length of the other leg in the z plane.

$$z = R_1 Z + z_0 \qquad Z = \frac{z - z_0}{R_1} \qquad (2.1)$$

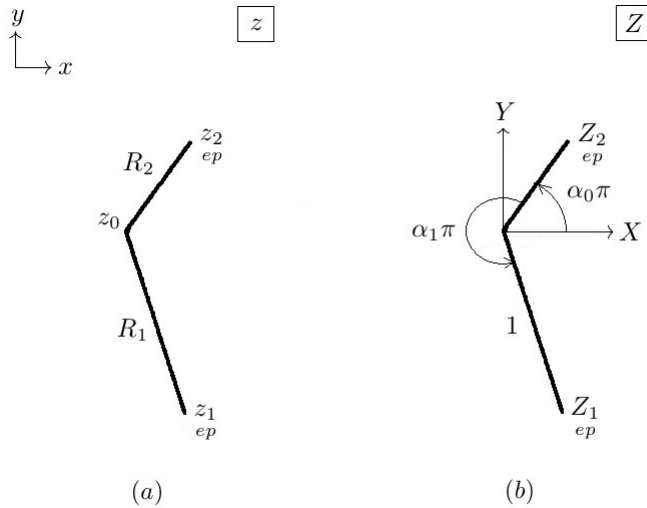


Figure 2.1: The slot in global (a) and local (b) coordinates.

The mapping from the upper half plane $\Im\zeta \geq 0$, shown in Figure 2.2(b), onto the slot in the Z plane shown in Figure 2.2(a) involves several parameters related to the geometry of the slot.

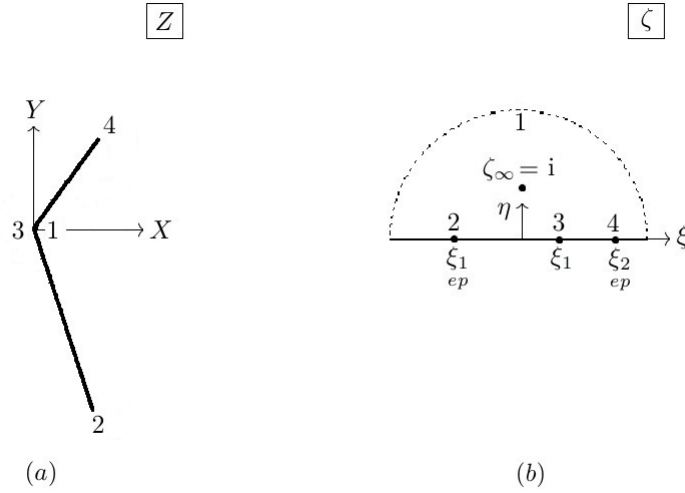


Figure 2.2: The slot in the Z plane (a) and the upper half plane ζ (b).

Points 1-4 are labelled in the Z plane, starting on the positive real side of the origin, going around the slot with the domain on the left. These points correspond to points 1-4 along the real axis of the upper half plane. Point 1 is at the origin in the Z plane, and we choose the mapping such that it corresponds to infinity in the upper half plane. Points 2 and 4 are the location of the endpoints in each plane; these points do not enter the transformation, but are labelled to help illustrate the mapping. Point 3 is also at the origin in the Z plane, on the other side of the slot, and corresponds to ξ_1 in the upper half plane. Infinity in the Z plane is chosen to map onto $\zeta = i$ in the upper half plane. The angle between the two legs, as shown in figure 2.1(b), is $\alpha_1\pi$. $\alpha_0\pi$ governs the orientation of the slot. The size of the slot is scaled by a factor A in the z plane and by $\frac{A}{r}$ in the Z plane, where $\frac{A}{r} = A/R_1$. The mapping function is then written in such a way that the boundary conditions are met.

The mapping function is that of a polygon that contains the origin and not infinity from Strack (1989).

$$Z = |A| e^{i\alpha_0} \frac{(\zeta - \xi_1)^{\alpha_1}}{(\zeta + i)(\zeta - i)} \quad (2.2)$$

One degree of freedom remains, ξ_1 , which will be determined from the ratio of the lengths of the legs. Identical slots can be made using different sets of parameters, this is shown and explained in appendix A.

Boundary Conditions of the Function $Z(\zeta)$

We check that the boundary conditions are met, i.e., that the real axis of the upper half plane is mapped onto the slot. The following equations are the mathematical statement of the boundary conditions.

$$\eta = 0 \quad -\infty < \xi < \xi_{1 \underset{ep}{}} \quad Z = |Z| e^{i(\alpha_0 + \alpha_1)\pi} \quad 0 < |Z| < |Z_{1 \underset{ep}{}}| \quad (2.3)$$

$$\eta = 0 \quad \xi_{1 \underset{ep}{}} < \xi < \xi_1 \quad Z = |Z| e^{i(\alpha_0 + \alpha_1)\pi} \quad |Z_{1 \underset{ep}{}}| < |Z| < 0 \quad (2.4)$$

$$\eta = 0 \quad \xi_1 < \xi < \xi_{2 \underset{ep}{}} \quad Z = |Z| e^{i\alpha_0\pi} \quad 0 < |Z| < |Z_{2 \underset{ep}{}}| \quad (2.5)$$

$$\eta = 0 \quad \xi_{2 \underset{ep}{}} < \xi < \infty \quad Z = |Z| e^{i\alpha_0\pi} \quad |Z_{2 \underset{ep}{}}| < |Z| < 0 \quad (2.6)$$

For the case of the identical slot made with different sets of parameters, the boundary conditions will be slightly different; this is shown and explained in appendix A.

Location of the Endpoints

The end points of the legs, points $Z_{1 \underset{ep}{}}$ and $Z_{2 \underset{ep}{}}$ are points where the derivative of the function $Z = Z(\zeta)$ is zero; the orientation of the increment dZ changes by 180 degrees, this implies a sign change and the magnitude must be zero at the

point of reversal of direction. Figure 2.3 shows how the direction of dZ reverses at the end points while the direction of $d\zeta$ remains the same.

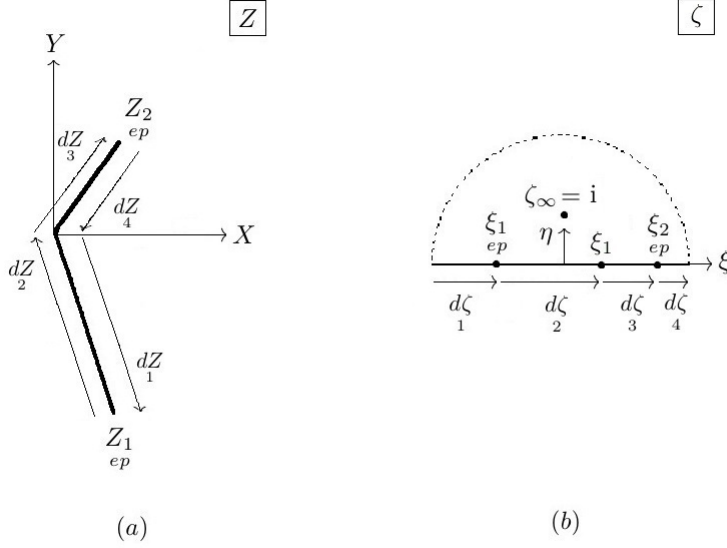


Figure 2.3: dZ (a) and $d\zeta$ (b).

We will find expressions for the coordinates of the points in the upper half plane by setting $dZ/d\zeta = 0$. We will need to obtain an expression for $dZ/d\zeta$ and will use logarithmic differentiation in order to facilitate the process. First, we take the logarithm of the function

$$\ln Z = \ln \left| \frac{A}{r} \right| + i\alpha_0 + \sum_{m=1}^3 \alpha_m \ln(\zeta - \xi_m) \quad (2.7)$$

where

$$\xi_2 = i \quad \xi_3 = -i \quad \alpha_2 = \alpha_3 = -1 \quad (2.8)$$

and then we differentiate this function with respect to ζ .

$$\frac{d \ln Z}{d\zeta} = \frac{Z'(\zeta)}{Z(\zeta)} = \sum_{m=1}^3 \frac{\alpha_m}{\zeta - \xi_m} \quad (2.9)$$

The function $Z(\zeta)$ is unequal to zero at the points where $Z'(\zeta)$ is zero, because the endpoints are not at the origin in the Z plane. The zeros of the derivative of the mapping function are found from

$$\frac{\alpha_1}{\zeta - \xi_1} - \frac{1}{\zeta - i} - \frac{1}{\zeta + i} = 0 \quad (2.10)$$

or

$$(\alpha_1 - 2)\zeta^2 + 2\xi_1\zeta + \alpha_1 = 0 \quad (2.11)$$

The mapping is defined such that the slot in the Z plane corresponds to the real axis of the upper half plane, therefore the endpoints in the upper half plane must be real. The locations of the end points in the upper half plane are given by

$$\xi_{j,ep} = \frac{-\xi_1 \pm \sqrt{\xi_1^2 - (\alpha_1 - 2)\alpha_1}}{\alpha_1 - 2} \quad j = 1, 2 \quad (2.12)$$

$\xi_{1,ep}$ is defined to correspond with the endpoint of the longer leg, with length R_1 ; the longer leg has unit length in the Z plane. If the lengths of the two legs are equal ($\xi_1 = 0$), either endpoint can be defined as $\xi_{1,ep}$. The points in the Z plane that correspond to these roots are

$$Z_{1,ep} = Z\left(\xi_{1,ep}\right) \quad Z_{2,ep} = Z\left(\xi_{2,ep}\right) \quad (2.13)$$

Equations (2.12) and (2.13) contain the quantities $\xi_{1,ep}$ and $\xi_{2,ep}$, which depend upon the unknown parameters A , α_0 , ξ_1 and α_1 . These equations form a non-linear system that need to be solved to obtain values for the parameters for any given geometry.

3 MAPPING THE ELEMENT ONTO THE UNIT CIRCLE IN THE χ PLANE

We will use an analogy to obtain an element of the desired shape. Note that this element is different from the slot, which is used as an aid to construct the element. The analogy is that of groundwater flow from infinity toward the two-legged slot. For a selected geometry of the slot there are a family of equipotentials that may be chosen for the elements shape. The choice will be based upon the shape of the feature to be represented with the element. As an example, an equipotential resulting from such a flow is shown in figure 3.1(a). Complete flow nets are located in appendix C.

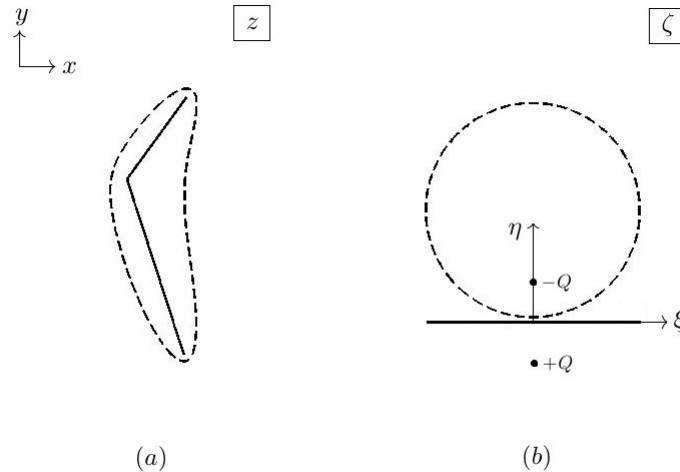


Figure 3.1: Equipotentials in the z plane (a) and the upper half plane (b).

The mapping will involve an analogous complex potential, Ω_{map} , for flow from infinity toward the two-legged slot. As infinity in the Z plane corresponds to $\zeta = i$ in the upper half plane, this corresponds in the latter plane to flow from $\zeta = i$ through the real axis using the method of images, Strack (1989). A well

of recharge Q is placed at $\zeta = i$ and a image well is symmetrically placed in the lower half plane at $\zeta = -i$ with discharge Q . The recharge well will create radial flow away from the point $\zeta = i$, creating circular equipotentials about that point, Strack (1989 pg.234). The image well will create radial flow towards the point $\zeta = -i$ and cause the circular equipotentials that were centered about $\zeta = i$ to become centered at values $\eta > i$. The function that maps the boundary of the element onto a circle in the upper half plane shown in Figure 3.1(b) has the form of a complex potential for flow from a recharge well at $\zeta = i$ to an image well at $\zeta = -i$.

$$\Omega_{map} = \frac{Q}{2\pi} \ln \frac{\zeta + i}{\zeta - i} \quad (3.1)$$

The boundary of the element corresponds to a value of the potential greater than zero because flow is towards the slot.

The discharge potentials of the well and image well cancel along the real axis of the upper half plane, $\ln((\zeta + i)/(\zeta - i))$ is imaginary, therefore along the slot

$$\Phi_{map} = \Re \Omega_{map} = 0 \quad (3.2)$$

We now wish to map the element onto the exterior of the unit circle in the χ plane shown in Figure 3.2(b). Having the element mapped onto the unit circle will be beneficial in the next sections as it will allow a direct method for evaluating contour integrals. One parameter is required for this transformation, ν , a radius in the χ plane that is less than one. Note, when mapping the upper half plane onto the exterior of the two-legged slot, shown in figure 2.2, the real axis of the upper half plane was chosen to be along the slot, and the following points were chosen: $\zeta = i$ was mapped to infinity in the Z plane, infinity in the upper half plane was mapped to point 1, and ξ_1 was mapped to point 3. ξ_1 was the degree of freedom in equation (2.2) that was determined by the ratio of the

lengths of the legs. Now, infinity in the χ plane corresponds to infinity in the Z plane, as we are mapping the slot onto the exterior of the unit circle, and will also correspond to $\zeta = i$ in the upper half plane. Point 1, infinity in the upper half plane is chosen to map onto $\chi = -i$. The origin in the upper half plane is chosen to map onto $\chi = i$ and is denoted as point 2^* . This is shown in figure 3.2. The mapping function is then written in a way such that the boundary conditions are met.

$$\frac{\chi}{\nu} = \frac{2}{\zeta - i} - i \quad (3.3)$$

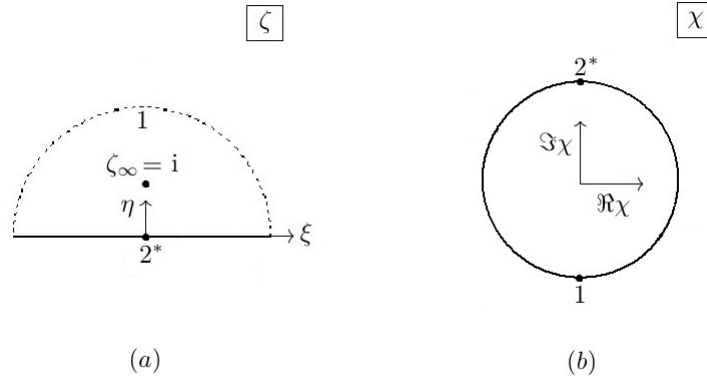


Figure 3.2: The upper half plane (a) and the χ plane (b).

Boundary Conditions of the Function $\chi(\zeta)$

We check that the boundary conditions are met, i.e., that the real axis of the upper half plane is mapped onto the unit circle in the χ plane. The following equations are the mathematical statement of the boundary conditions.

$$\eta = 0 \quad -\infty < \xi < 0 \quad \frac{\chi}{\nu} = e^{i\theta} \quad \frac{\pi}{2} < \theta < -\frac{\pi}{2} \quad (3.4)$$

$$\eta = 0 \quad 0 < \xi < \infty \quad \frac{\chi}{\nu} = e^{i\theta} \quad -\frac{\pi}{2} < \theta < \frac{\pi}{2} \quad (3.5)$$

The analogous complex potential can be written in terms of χ by using (3.1) to express ζ in terms of χ , then substituting that expression into (3.3).

Replacing the numerator in the log term with

$$\zeta + i = \frac{2}{\frac{\chi}{\nu} + i} + 2i = 2 \frac{1 + i(\frac{\chi}{\nu} + i)}{\frac{\chi}{\nu} + i} = 2i \frac{\frac{\chi}{\nu}}{\frac{\chi}{\nu} + i} \quad (3.6)$$

and the denominator with

$$\zeta - i = \frac{2}{\frac{\chi}{\nu} + i} \quad (3.7)$$

the analogous complex potential becomes

$$\Omega_{map} = \frac{Q}{2\pi} \ln \left(i \frac{\chi}{\nu} \right) = \frac{Q}{2\pi} \ln \frac{\chi}{\nu} + \frac{Q}{4} i\pi \quad (3.8)$$

Flow from infinity in the z plane towards the slot corresponds with flow from infinity in the χ plane towards the unit circle. Therefore, any circle in the χ plane centred at the origin with radius greater than one corresponds to an equipotential in the z plane around the slot. This is illustrated in figure 3.3. Complete flow nets of the analogous complex potential in the z , ζ and χ planes are located in appendix C. If the potential for the desired shape is Φ_{map} , then $\Phi_{map} > 0$, the flow is to the slot and we have

$$\frac{2\pi \Phi_{map}}{Q} = \ln \left| \frac{\chi}{\nu} \right| \quad (3.9)$$

or

$$\left| \frac{\chi}{\nu} \right| = e^{\frac{2\pi \Phi_{map}}{Q}} \quad (3.10)$$

The latter equation makes it possible to choose the parameter ν such that the shape corresponds to the unit circle in the χ plane, i.e.,

$$\nu = e^{-\frac{2\pi \Phi_0}{Q}} \quad (3.11)$$

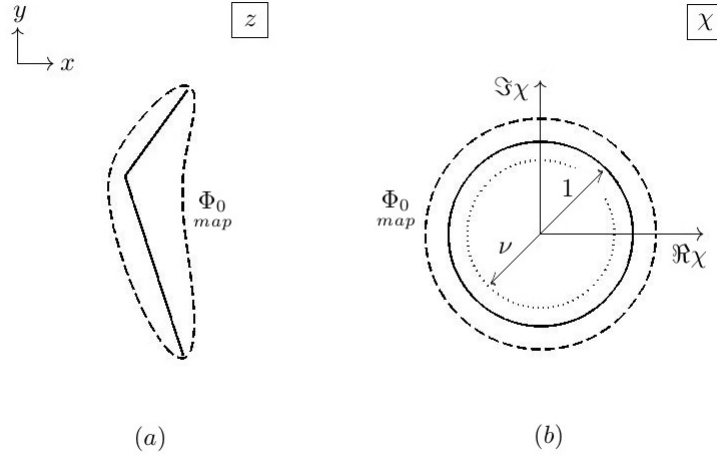


Figure 3.3: Equipotentials in the z plane (a) and in the χ plane (b) with corresponding circle of radius ν .

With Q held constant the desired equipotential, Φ_0 , can be chosen from the family of equipotentials for a selected geometry of the two-legged slot. The members of the family of equipotentials progress radially away from the slot, gradually losing the original definition in shape created by the geometry of the two legs. The further away the equipotential is from the two-legged slot, the more circular the contours of the equipotentials will become. Figure 3.4 shows a family of equipotentials with corresponding values of ν . More examples can be seen in appendix A.

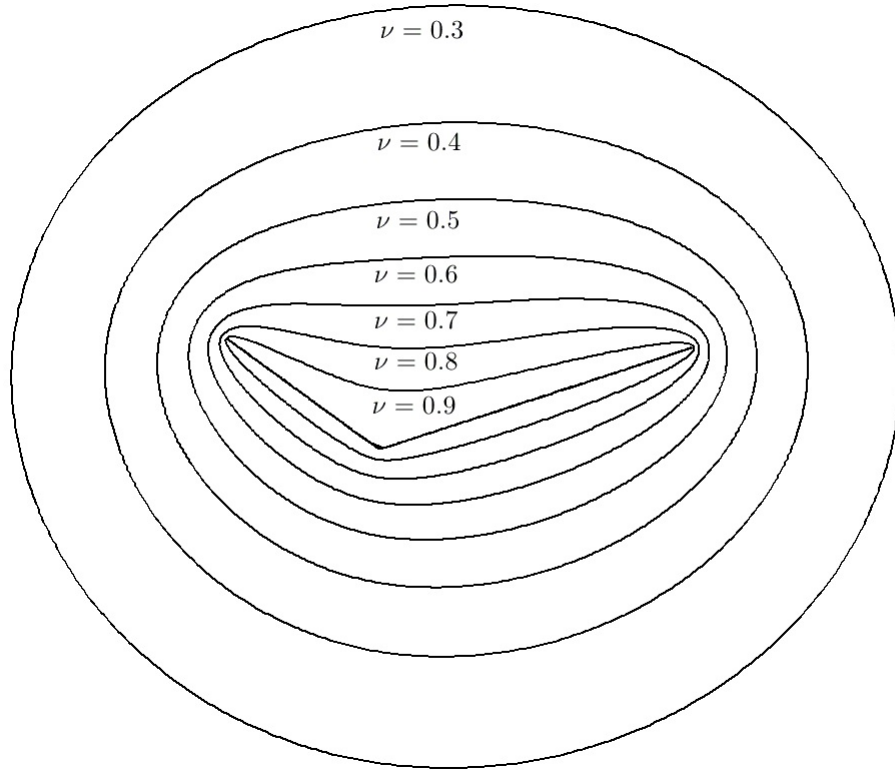


Figure 3.4: A two-legged slot with contours of equipotentials with corresponding values of ν from 0.3-0.9.

As ν approaches one the elements shape approaches the two-legged slot. As ν approaches zero the elements shape approaches a circle.

For the case that $\nu = 1$ the shape is that of the two-legged slot and can be represented more easily using line segments. For the case that $\alpha_1 = 1$ it is simpler to use the mapping for an ellipse, also when the elements shape becomes nearly circular, it is recommended to use the mapping for a circle. The mappings for lines, ellipses and circles do not require the mapping function to be written as multiple series expansions that require reversion and analytic continuation. These requirements will be explained in the next section.

4 SERIES EXPANSIONS

Groundwater flow problems in the complex coordinate system z will have their coordinates transformed into the χ plane where the problems are solved; afterward, the expressions for the complex potential need to be evaluated at points given in the physical plane $z = x + iy$, but not in terms of χ . Thus, the inverse transformation is needed, i.e., the transformation that will yield χ as a function of z . The work presented in this section is concerned with obtaining the inverse transformations using series expansions and their inverse. We cannot inverse the mapping function $Z(\zeta)$ explicitly; we will circumvent this difficulty by writing the mapping function as series expansions in a form such that the reversion of series is possible using the Lagrange inversion theorem.

The mapping for the two-legged slot is a transformation with piecewise constant argument, Strack (1989). The transformation has the property that its argument remains constant along each interval of the real axis of the upper half plane, $\Im\zeta = 0$, and changes by an amount related to the geometry of the slot at the corner points. It may be noted that the argument of $Z(\zeta)$ does not change at the endpoints, which therefore do not enter explicitly into the transformation. However, the argument of the derivative of the mapping function $dZ/d\zeta$ changes at both the corner points and endpoints as shown in figure 2.3.

As the increment dZ passes the location of the endpoints, from one side of the slot to the other, the argument changes by an amount equal to 2π . As the increment dZ passes the location of corner point one the argument changes by $\alpha_1\pi$, and at corner point two the change is $(2 - \alpha_1)\pi$. As the increment $d\zeta$ passes the corresponding location of the corner points and endpoints along the real axis the argument remains constant and is equal to π . The differences in the argument of the derivative of the mapping function at the endpoints and

corner points will create singularities at those points. For example, the change in argument at the endpoints results in a square root singularity, as $\sqrt{e^{i2\theta}} = e^{i\theta}$. The square root is a multivalued function therefore there will be branch cuts along the legs separating the desired roots from the others. There is a similar behaviour at the corner points resulting in singularities with a power that is a rational number. Because of the singularities and branch cuts, the inverse mapping will have to be in pieces.

The domain will be divided into sub domains with areas limited by the location of the singularities and branch cuts. Series expansions will be constructed to be valid within each subsection of the domain. Any analytic function can be expanded about a point in terms of a series expansion that converges inside any circle about the point that does not contain singularities. In practice, convergence is also limited by numerical accuracy, which is taken into consideration when dividing the domain into subsections for each expansion. We will construct a total of five series expansions and reversion to obtain inverse mappings for the entire domain that includes a single element. All of the expansions will be in the form of an infinite series of positive powers starting at one, so that the reversion process will be the same for each series.

We first construct the far-field expansion to represent $Z(\chi)$ outside of the unit circle in the Z plane and will extend to infinity. This corresponds to the area outside of a circle centered at z_0 with radius R_1 in global coordinates, and is shown in figure 4.1. The reversion of the series will be used to get the function $\chi(Z)$.

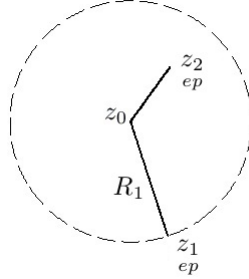


Figure 4.1: Domain of the far field expansion, out side the dashed line.

The second and third expansions will represent $Z(\zeta)$ inside a circle centered at each endpoint. These expansions will yield the functions $\zeta(Z)$ after reversion. The radius of the circles which the endpoint expansions will be valid in is dependent upon the geometry of the two-legged slot and will be explained in detail in section 4.2, Expansions About the Endpoints. Two examples of the domains of validity of the endpoint expansions are shown in figure 4.2.

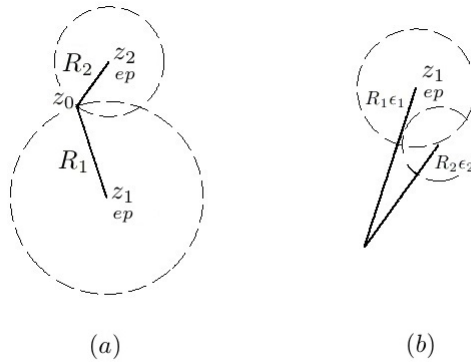


Figure 4.2: Domains for the endpoint expansions, inside the dashed lines.

The fourth and fifth expansions to represent the function $Z(\zeta)$ will be about each corner point, valid inside circular arcs between the legs with radii of the shorter leg. These expansions will yield the functions $\zeta(Z)$ after reversion. Figure 4.3 illustrates the area in the z plane for which these expansions will be valid.

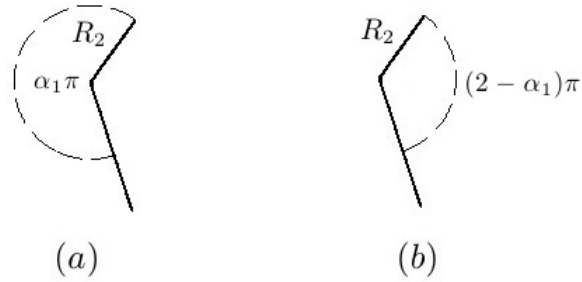


Figure 4.3: The domain for the corner point expansions, inside the dashed arcs.

We have the inverse mapping for most of the domain with the series expansions and reversion for the far field, endpoints and corner points. However, there is still a portion of a ring between the domains of the corner point expansions and the far field which is not completely covered by the expansions about the endpoints. This is illustrated in figure 4.4.

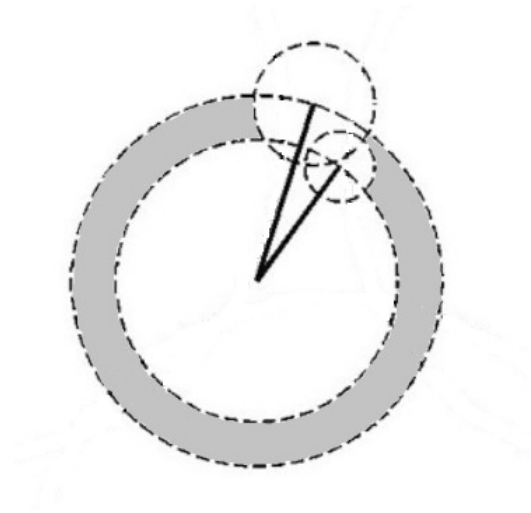


Figure 4.4: The ring between the corner point expansions and the far field (shaded) along with the sub domains for each expansion.

The example corresponds with figure 4.2(b). It is chosen because it is a more

difficult case than the example in figure 4.2(a); there is less overlap, or union, of the sub domains. Analytic continuation will be used to expand the far field reversion, $\chi(Z)$, into the rest of the domain that has not been covered by the other expansions.

In general, three analytic continuations along with the five series expansions and reversions will be required to obtain the inverse mappings over the entire domain for a single element. With the expansions in place, a method for evaluating the inverse mapping functions will be constructed so that given any point z the correct expansion can be chosen to find the corresponding value of χ . Each series expansion will be explained in detail in the following sections, along with the methods for series reversion and analytic continuation.

4.1 Far Field Expansion

We wish to construct a series expansion to represent the function $Z(\chi)$ that will be valid outside of a circle containing the singularities at the end points. This is a circle centered at z_0 with radius of the longer leg R_1 , which corresponds in the Z plane to a circle centered at the origin with radius of unit length.

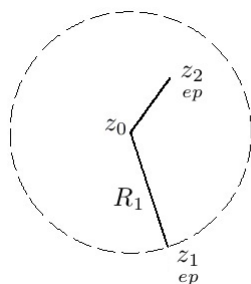


Figure 4.1.1: Domain of the far field expansion, out side the dashed line.

The expansion will be written in the form of an infinite series of positive powers starting at one, and the reversion of the series will be performed using the Lagrange inversion formula. The function $Z = Z(\chi)$ is holomorphic outside the unit circle in the χ plane and thus can be expanded in a series. We choose the reciprocal of the mapping function as it requires less steps to get into the desired form which is suitable for reversion. The series is as follows, where b_j are complex coefficients.

$$\frac{1}{Z} = \sum_{j=1}^{\infty} b_j \chi^{-j} \quad (4.1.1)$$

To obtain positive powers we replace

$$\Xi = \frac{1}{Z} \quad \psi = \frac{1}{\chi} \quad (4.1.2)$$

which gives the series in the desired form.

$$\boxed{\Xi = \sum_{j=1}^{\infty} b_j \psi^j} \quad (4.1.3)$$

Because the mapping function is holomorphic out side of the unit circle in the χ plane, the coefficients b_j for the expansion (4.1.3) can be solved for in the manner of a Fourier series such that

$$b_j = \frac{1}{2\pi} \oint \Xi(\theta) e^{-ij\theta} d\theta \quad j = 1, 2, \dots \quad (4.1.4)$$

where

$$\Xi = \frac{(\zeta + i)(\zeta - i)}{|A| e^{i\alpha_0} (\zeta - \xi_1)^{\alpha_1}} \quad (4.1.5)$$

$$\zeta = \frac{\frac{\chi}{\nu} + i}{\nu} + i \quad (4.1.6)$$

and along the unit circle

$$\chi = e^{i\theta} \quad (4.1.7)$$

When substituting equations (4.1.5), (4.1.6) and (4.1.7) into (4.1.4) it is important not to over simplify the mapping function. If the ratio of $(\chi + i)/(\chi - i)$, where $\chi = e^{i\theta}$, is written as a tangent of theta

$$\frac{\chi + i}{\chi - i} = i \tan\left(\frac{\theta}{2} - \frac{\pi}{4}\right) \quad (4.1.8)$$

the function will be undefined at $\theta = 3\pi/2$ and $\theta = -\pi/2$ and there will be a branch cut interrupting the mapping, resulting in part of the elements shape

being on the wrong sheet, as shown in figure 4.1.2.

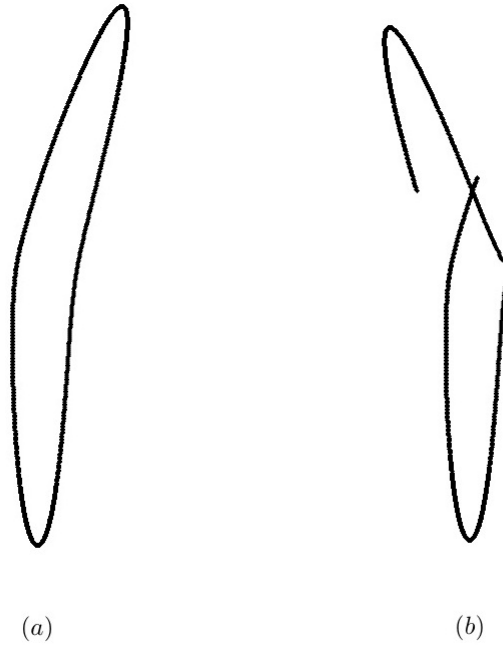


Figure 4.1.2: An element (a) and an element with an improper branch cut (b).

With the series (4.1.3) in the desired form, and the coefficients known, the reversion of the series can be obtained. The series after reversion will have the form

$$\psi = \sum_{n=1}^{\infty} c_n \Xi^n \quad (4.1.9)$$

where the coefficients can be found using the method described in section 5, Series Reversion.

4.2 Expansions About the Endpoints

We wish to construct series expansions representing the mapping function $Z = Z(\zeta)$ centered at each endpoint. The expansions will be valid inside a circle with a maximum radius governed by the distance to the singularity at the other endpoint, or the singularities at the corner points. The expansions are valid within a circle with a maximum radius of the length of the leg corresponding to that endpoint. The maximum radius for the expansion about z_1 is R_1 , and for z_2 is R_2 , each domain being limited by the singularities at the corner points. For cases where $3/2 < \alpha_1 < 1/2$ the maximum radius of each expansion will be decreased. The expansion about the end point of the longer leg is then valid within a circle of maximum radius equal to the distance between the endpoints, the distance to the nearest singularity. In the z plane this distance is $R_1\epsilon_1 = |z_1 - z_2|$. The expansion about the shorter legs endpoint will be numerically accurate within a circle with a maximum radius that is equal to the shortest distance to the other leg, the distance to the branch cut from the other endpoint. In the z plane this distance is $R_2\epsilon_2$, where $\epsilon_2 = \sin \alpha_1$. An example of each case can be seen in figure 4.2.1.

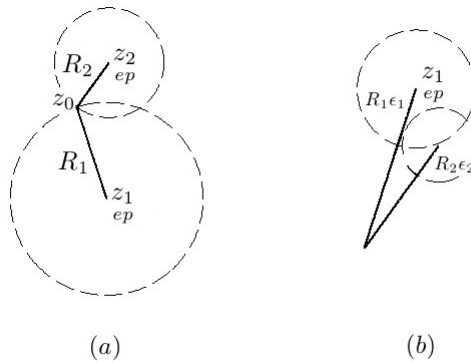


Figure 4.2.1: Domains for the endpoint expansions, inside the dashed lines.

The expansion will be written as an infinite series of positive powers starting at one so that the reversion of the series can be obtained in the same manner as the other expansions. This will be done by representing the mapping function with a set of Taylor series. The mapping function

$$Z = |A|_r e^{i\alpha_0} \frac{(\zeta - \xi_1)^{\alpha_1}}{(\zeta + i)(\zeta - i)} \quad (4.2.1)$$

must be rewritten into a form that can be expanded about an end point, ξ_{ep} , in the upper half plane. ξ_{ep} is added and subtracted in the numerator and denominator so that there is a $(\zeta - \xi_{ep})$ term where ever ζ is present, as the expansion will be in terms of $(\zeta - \xi_{ep})$

$$Z = |A|_r e^{i\alpha_0} \frac{\left[\left(\zeta - \xi_{ep} \right) + \left(\xi_{ep} - \xi_1 \right) \right]^{\alpha_1}}{1 + \left(\zeta - \xi_{ep} + \xi_{ep} \right)^2} \quad (4.2.2)$$

and the terms are reorganized.

$$Z = |A|_r e^{i\alpha_0} \frac{\left[1 + \frac{\zeta - \xi_{ep}}{\xi_{ep} - \xi_1} \right]^{\alpha_1} \left(\xi_{ep} - \xi_1 \right)^{\alpha_1}}{1 + \left[1 + \frac{\zeta - \xi_{ep}}{\xi_{ep}} \right]^2 \xi_{ep}^2} \quad (4.2.3)$$

Both the numerator and denominator have a bracketed term that can be written as $(1 + t)^\alpha$ which there is a Taylor series expansion for

$$(1 + t)^\alpha = \sum_{n=0}^{\infty} \binom{\alpha}{n} t^n \quad (4.2.4)$$

with generalized binomial coefficients

$$\binom{\alpha}{n} = \prod_{k=1}^n \frac{\alpha - k + 1}{k} \quad (4.2.5)$$

In the numerator

$$t = \left(\frac{\zeta - \xi}{\xi - \xi_1} \right)_{ep} \quad \alpha = \alpha_1 \quad (4.2.6)$$

and in the denominator

$$t = \left(\frac{\zeta - \xi}{\xi} \right)_{ep} \quad \alpha = 2 \quad (4.2.7)$$

Substituting the bracketed terms in (4.2.3) for their corresponding Taylor series the mapping function becomes

$$Z = |A|_r e^{i\alpha_0} \frac{\left(\frac{\zeta - \xi}{\xi - \xi_1} \right)_{ep}^{\alpha_1} \sum_{n=0}^{\infty} \binom{\alpha_1}{n} \left(\frac{\zeta - \xi}{\xi - \xi_1} \right)_{ep}^n}{1 + \xi_{ep}^2 \sum_{n=0}^{\infty} \binom{2}{n} \left(\frac{\zeta - \xi}{\xi} \right)_{ep}^n} \quad (4.2.8)$$

which can be simplified to

$$Z = \frac{\sum_{n=0}^{\infty} a_n \left(\frac{\zeta - \xi}{\xi} \right)_{ep}^n}{\sum_{n=0}^{\infty} b_n \left(\frac{\zeta - \xi}{\xi} \right)_{ep}^n} \quad (4.2.9)$$

where

$$a_n = |A|_r e^{i\alpha_0} \binom{\alpha_1}{n} \left(\frac{\zeta - \xi}{\xi} \right)_{ep}^{\alpha_1 - n} \quad n = 0, 1, 2, \dots \quad (4.2.10)$$

$$b_0 = 1 + \binom{2}{0} \xi_{ep}^2 \quad (4.2.11)$$

and

$$b_n = \binom{2}{n}_{ep} \xi^{2-n} \quad n = 1, 2, \dots \quad (4.2.12)$$

To simplify further, the quotient of two series can be written as a single series, Knuth (1998).

$$Z = \frac{\sum_{n=0}^{\infty} a_n \left(\zeta - \frac{\xi}{ep} \right)^n}{\sum_{n=0}^{\infty} b_n \left(\zeta - \frac{\xi}{ep} \right)^n} = \sum_{n=0}^{\infty} c_n \left(\zeta - \frac{\xi}{ep} \right)^n \quad (4.2.13)$$

where

$$c_n = \frac{a_n - \sum_{k=0}^{n-1} c_k b_{n-k}}{b_0} \quad n = 0, 1, 2, \dots \quad (4.2.14)$$

The constant is equal to the location of the end point, $c_0 = Z_{ep}$ because we are expanding about that point. The first coefficient is zero, $c_1 = 0$, because the first derivative of the mapping function is zero at the endpoints, therefore

$$Z - Z_{ep} = \sum_{n=2}^{\infty} c_n \left(\zeta - \frac{\xi}{ep} \right)^n \quad (4.2.15)$$

We now have an infinite series of positive powers that starts at two, however, it needs to start at one. The square root singularities at the endpoints will be built into the expansion by writing it in terms of $\sqrt{Z - Z_{ep}}$. This will be mandatory for the use of the Lagrange inversion theorem. The following steps are made to get the expansion into the required form. First, equation (4.2.15) is rewritten as

$$Z - Z_{ep} = \left(\zeta - \frac{\xi}{ep} \right)^2 \sum_{n=2}^{\infty} c_n \left(\zeta - \frac{\xi}{ep} \right)^{n-2} \quad (4.2.16)$$

and the coefficients are renamed $d_n = c_{n+2}$ for all $n \geq 0$.

$$Z - \frac{Z}{ep} = \left(\zeta - \frac{\xi}{ep} \right)^2 \sum_{n=0}^{\infty} d_n \left(\zeta - \frac{\xi}{ep} \right)^n \quad (4.2.17)$$

Now the series will be raised to the one half power. The formula to do so requires that the first coefficient be equal to one; both sides are divided by d_0 .

$$\frac{Z - \frac{Z}{ep}}{d_0} = \left(\zeta - \frac{\xi}{ep} \right)^2 \sum_{n=0}^{\infty} \frac{d_n}{d_0} \left(\zeta - \frac{\xi}{ep} \right)^n \quad (4.2.18)$$

The coefficients are renamed $v_n = d_n/d_0$ for all $n \geq 0$, and the square root is taken.

$$\sqrt{\frac{Z - \frac{Z}{ep}}{d_0}} = \left(\zeta - \frac{\xi}{ep} \right) \left(\sum_{n=0}^{\infty} v_n \left(\zeta - \frac{\xi}{ep} \right)^n \right)^{1/2} \quad (4.2.19)$$

A series raised to the one half power can be written as a new series, Knuth (1998). This keeps the series in a standard form, with powers that are integers.

$$\left(\sum_{n=0}^{\infty} v_n \left(\zeta - \frac{\xi}{ep} \right)^n \right)^{1/2} = \sum_{n=0}^{\infty} w_n \left(\zeta - \frac{\xi}{ep} \right)^n \quad (4.2.20)$$

Where $w_0 = v_0^{1/2} = 1$, and for all $n \geq 1$

$$w_n = \sum_{k=1}^n \left(\binom{1/2+1}{n} k - 1 \right) v_k w_{n-k} \quad (4.2.21)$$

Substituting the new series in (4.2.20) into (4.2.19) we have

$$\sqrt{\frac{Z - \frac{Z}{ep}}{d_0}} = \left(\zeta - \frac{\xi}{ep} \right) \sum_{n=0}^{\infty} w_n \left(\zeta - \frac{\xi}{ep} \right)^n \quad (4.2.22)$$

Multiplying through by $\sqrt{d_0}$

$$\sqrt{Z - \frac{Z}{ep}} = \sqrt{d_0} \left(\zeta - \frac{\xi}{ep} \right) \sum_{n=0}^{\infty} w_n \left(\zeta - \frac{\xi}{ep} \right)^n \quad (4.2.23)$$

and replacing the coefficients and the square root of the constant with

$$u_n = \sqrt{d_0} w_{n-1} \quad n = 1, 2, \dots \quad (4.2.24)$$

The mapping function can finally be written as

$$\boxed{\sqrt{Z - \frac{Z}{ep}} = \sum_{n=1}^{\infty} u_n \left(\zeta - \frac{\xi}{ep} \right)^n} \quad (4.2.25)$$

We now have an expansion about the endpoints in the form of an infinite series of positive powers starting at one with known coefficients. Upon reversion the series will become

$$\left(\zeta - \frac{\xi}{ep} \right) = \sum_{n=1}^{\infty} a_n \left(\sqrt{Z - \frac{Z}{ep}} \right)^n \quad (4.2.26)$$

where the coefficients can be found using the method in the section on series reversion. Note, when evaluating the square root in the reversion the branch cuts must be treated properly; this is explained in appendix B.

4.3 The Expansion About Corner Point One

We wish to construct a series expansion representing the mapping function $Z = Z(\zeta)$ about corner point one. The expansion will be valid within a circular arc on one side of the slot centered at z_0 with radius of the shorter leg, R_2 . The radius of the expansion is limited by the singularity at z_2 , the end of the shorter leg. The circular arc length is limited by the angle $\alpha_1\pi$, which is bounded by the branch cuts that are along each leg. A diagram showing an example of the area which the first corner point expansion will be valid can be seen in figure 4.3.1.



Figure 4.3.1: The domain for the corner point one expansion, inside the dashed arc.

The expansion will be written as an infinite series of positive powers starting at one so that the reversion of the series can be obtained in the same manner as the other expansions. This will be done by representing the mapping function with a set of Taylor series. The mapping function

$$Z = |A|_r e^{i\alpha_0} \frac{(\zeta - \xi_1)^{\alpha_1}}{(\zeta + i)(\zeta - i)} \quad (4.3.1)$$

must be rewritten into a form that can be expanded about the corner point ξ_1 in the upper half plane. First, ξ_1 is added and subtracted in the denominator

so that there is a $(\zeta - \xi_1)$ term where ever ζ is present, as the expansion will be in terms of $(\zeta - \xi_1)$.

$$Z = |A|_r e^{i\alpha_0} \frac{(\zeta - \xi_1)^{\alpha_1}}{(\zeta - \xi_1 + \xi_1 + i)(\zeta - \xi_1 + \xi_1 - i)} \quad (4.3.2)$$

The rational root singularity at the corner point will be built into the expansion by writing it in terms of Z^{1/α_1} . The function is raised to the $1/\alpha_1$ power

$$Z^{1/\alpha_1} = \left(|A|_r e^{i\alpha_0}\right)^{1/\alpha_1} (\zeta - \xi_1) [(\zeta - \xi_1) + (\xi_1 + i)]^{-1/\alpha_1} [(\zeta - \xi_1) + (\xi_1 - i)]^{-1/\alpha_1} \quad (4.3.3)$$

and the terms are reorganized.

$$\begin{aligned} Z^{1/\alpha_1} = & \left(|A|_r e^{i\alpha_0}\right)^{1/\alpha_1} (\zeta - \xi_1) \left[1 + \frac{\zeta - \xi_1}{\xi_1 + i}\right]^{-1/\alpha_1} (\xi_1 \\ & + i)^{-1/\alpha_1} \left[1 + \frac{\zeta - \xi_1}{\xi_1 - i}\right]^{-1/\alpha_1} (\xi_1 - i)^{-1/\alpha_1} \end{aligned} \quad (4.3.4)$$

There are two bracketed terms which can be written as $(1 + t)^\alpha$ which there is a Taylor series expansion for with generalized binomial coefficients, as explained in equations (4.2.4) and (4.2.5). Substituting the bracketed terms with their respective Taylor series the mapping function becomes

$$\begin{aligned} Z^{1/\alpha_1} = & \left(|A|_r e^{i\alpha_0}\right)^{1/\alpha_1} (\zeta - \xi_1) \sum_{n=0}^{\infty} \binom{-1/\alpha_1}{n} \left[\frac{\zeta - \xi_1}{\xi_1 + i}\right]^n (\xi_1 \\ & + i)^{-1/\alpha_1} \sum_{n=0}^{\infty} \binom{-1/\alpha_1}{n} \left[\frac{\zeta - \xi_1}{\xi_1 - i}\right]^n (\xi_1 - i)^{-1/\alpha_1} \end{aligned} \quad (4.3.5)$$

which can be simplified to

$$Z^{1/\alpha_1} = \left(|A|_r e^{i\alpha_0}\right)^{1/\alpha_1} (\zeta - \xi_1) \sum_{n=0}^{\infty} a_n (\zeta - \xi_1)^n \sum_{n=0}^{\infty} b_n (\zeta - \xi_1)^n \quad (4.3.6)$$

where

$$a_n = \binom{-1/\alpha_1}{n} (\xi_1 + i)^{-1/\alpha_1 - n} \quad n = 0, 1, 2, \dots \quad (4.3.7)$$

and

$$b_n = \binom{-1/\alpha_1}{n} (\xi_1 - i)^{-1/\alpha_1 - n} \quad n = 0, 1, 2, \dots \quad (4.3.8)$$

To simplify further, the product of the two series in (4.3.6) can be written as a single series

$$\sum_{n=0}^{\infty} a_n (\zeta - \xi_1)^n \sum_{n=0}^{\infty} b_n (\zeta - \xi_1)^n = \sum_{n=0}^{\infty} c_n (\zeta - \xi_1)^n \quad (4.3.9)$$

and the coefficients can be found using the convolution rule, Knuth (1998).

$$c_n = \sum_{k=0}^n a_k b_{n-k} \quad n = 0, 1, 2, \dots \quad (4.3.10)$$

Substituting the new series from (4.3.9) into (4.3.6)

$$Z^{1/\alpha_1} = \left(|A|_r e^{i\alpha_0} \right)^{1/\alpha_1} (\zeta - \xi_1) \sum_{n=0}^{\infty} c_n (\zeta - \xi_1)^n \quad (4.3.11)$$

and replacing the constants and the coefficients with a new set of coefficients

$$d_n = \left(|A|_r e^{i\alpha_0} \right)^{1/\alpha_1} c_{n-1} \quad n = 1, 2, \dots \quad (4.3.12)$$

The expansion can now be written in its final form

$$\boxed{Z^{1/\alpha_1} = \sum_{n=1}^{\infty} d_n (\zeta - \xi_1)^n} \quad (4.3.13)$$

We now have an expansion about corner point one in the form of an infinite series of positive powers starting at one with known coefficients. Upon reversion the series will become

$$(\zeta - \xi_1) = \sum_{n=1}^{\infty} a_n \left(Z^{1/\alpha_1} \right)^n \quad (4.3.14)$$

where the coefficients can be found using the method in the section on series reversion. Note, when evaluating Z^{1/α_1} in the reversion, the expansion may need to be rotated to go between the branch cuts properly; this is explained in appendix B.

4.4 The Expansion About Corner Point Two

We wish to construct a series expansion representing the mapping function $Z = Z(\zeta)$ about corner point two. The expansion will be valid within a circular arc on the other side of the slot centered at z_0 with radius of the shorter leg, R_2 . The radius of the expansion is limited by the singularity at z_2 , the endpoint of the shorter leg. The circular arc length is limited by the angle $(2 - \alpha_1)\pi$, which is bounded by the branch cuts that are along each leg. A diagram showing an example of the area which the second corner point expansion will be valid can be seen in figure 4.4.1.

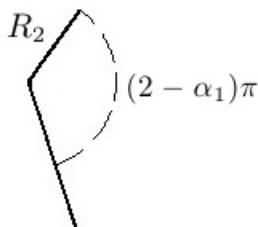


Figure 4.4.1: The domain for the corner point two expansion, inside the dashed arc.

The expansion will be written as an infinite series of positive powers starting at one so that the reversion of the series can be obtained in the same manner as the other expansions. This will be done by representing the mapping function with a Taylor series. The mapping function

$$Z = |A|_r e^{i\alpha_0} \frac{(\zeta - \xi_1)^{\alpha_1}}{(\zeta + i)(\zeta - i)} \quad (4.4.1)$$

must be rewritten into a form that can be expanded about the corner point ξ_1 in the upper half plane. First, ξ_1 is added and subtracted in the denominator

so that there is a $(\zeta - \xi_1)$ term where ever ζ is present, as the expansion will be in terms of $(\zeta - \xi_1)$.

$$Z = |A|_r e^{i\alpha_0} \frac{(\zeta - \xi_1)^{\alpha_1}}{(\zeta - \xi_1 + \xi_1 + i)(\zeta - \xi_1 + \xi_1 - i)} \quad (4.4.2)$$

Some intermediate variables are defined to simplify the following algebraic steps that will be used to get the mapping function into a form that may be represented with Taylor series.

$$t = \zeta - \xi_1 \quad B = \xi_1 - i \quad C = \xi_1 + i \quad D = |A|_r e^{i\alpha_0} \quad (4.4.3)$$

Note that B , C and D are all constants and t is the term that will be in the expansion. Substituting the new variables defined in (4.4.3) into (4.4.2) the mapping function becomes

$$Z = D \frac{t^{\alpha_1}}{(t + B)(t + C)} \quad (4.4.4)$$

Expanding the denominator

$$Z = D \frac{t^{\alpha_1}}{t^2 + Bt + Ct + BC} \quad (4.4.5)$$

collecting terms

$$Z = D \frac{t^{\alpha_1}}{t^2 + (B + C)t + BC} \quad (4.4.6)$$

and once again renaming variables

$$a = B + C \quad b = BC \quad (4.4.7)$$

the mapping function is simplified to

$$Z = D \frac{t^{\alpha_1}}{t^2 + at + b} \quad (4.4.8)$$

The rational root singularity at the corner point will be built into the expansion by writing it in terms of $Z^{1/(2-\alpha_1)}$. The following algebraic steps are made so that when the mapping function is raised to the $1/(2-\alpha_1)$ power the numerator can be excluded from the term that will be written as a Taylor series. The numerator and denominator are divided by t .

$$Z = D \frac{t^{\alpha_1-1}}{t + a + \frac{b}{t}} \quad (4.4.9)$$

Dividing the numerator and denominator by t again

$$Z = D \frac{t^{\alpha_1-2}}{1 + \frac{a}{t} + \frac{b}{t^2}} \quad (4.4.10)$$

and raising to the $1/(2-\alpha_1)$ power the mapping function becomes

$$Z^{1/(2-\alpha_1)} = D^{1/(2-\alpha_1)} \frac{t^{-1}}{\left(1 + \frac{a}{t} + \frac{b}{t^2}\right)^{1/(2-\alpha_1)}} \quad (4.4.11)$$

One more variable is introduced to further simplify the mapping function.

$$\tau = \frac{1}{t} \quad (4.4.12)$$

Substituting (4.4.12) into (4.4.11) the mapping function is now in a form that will be able to be expanded.

$$Z^{1/(2-\alpha_1)} = D^{1/(2-\alpha_1)} \tau [1 + a\tau + b\tau^2]^{-1/(2-\alpha_1)} \quad (4.4.13)$$

The bracketed term can be written as $(1 + T)^\alpha$ which there is a Taylor series

expansion for with generalized binomial coefficients, as explained in equations (4.2.4) and (4.2.5). Substituting the bracketed term with its respective Taylor series

$$Z^{1/(2-\alpha_1)} = D^{1/(2-\alpha_1)} \tau \sum_{n=0}^{\infty} \binom{-1/(2-\alpha_1)}{n} [a\tau + b\tau^2]^n \quad (4.4.14)$$

and renaming the generalized binomial coefficients

$$\alpha_n = \binom{-1/(2-\alpha_1)}{n} \quad (4.4.15)$$

the mapping function becomes

$$Z^{1/(2-\alpha_1)} = D^{1/(2-\alpha_1)} \tau \sum_{n=0}^{\infty} \alpha_n [a\tau + b\tau^2]^n \quad (4.4.16)$$

Which can be further simplified to

$$Z^{1/(2-\alpha_1)} = D^{1/(2-\alpha_1)} \tau \sum_{n=0}^{\infty} c_n \tau^n \quad (4.4.17)$$

where the constant is renamed

$$c_0 = \alpha_0 \quad (4.4.18)$$

and the coefficients are a combination of the α_n coefficients, the constants a and b , and another set of binomial coefficients. For all odd values of n

$$c_n = \sum_{k=0}^{(n-1)/2} \binom{n-k}{k} \alpha_{n-k} a^{n-2k} b^k \quad n = 1, 3, 5... \quad (4.4.19)$$

and for all even values of n

$$c_n = \alpha_{n/2} b^{n/2} + \sum_{k=0}^{(n/2)-1} \binom{n-k}{k} \alpha_{n-k} a^{n-2k} b^k \quad n = 2, 4, 6... \quad (4.4.20)$$

where the binomial coefficients are

$$\binom{m}{k} = \frac{m!}{k!(m-k)!} \quad (4.4.21)$$

Now the mapping function can be written in its final form

$$Z^{1/(2-\alpha_1)} = \sum_{n=1}^{\infty} d_n \tau^n \quad (4.4.22)$$

or

$$\boxed{Z^{1/(2-\alpha_1)} = \sum_{n=1}^{\infty} d_n \left(\frac{1}{\zeta - \xi_1} \right)^n} \quad (4.4.23)$$

where

$$d_n = D^{1/(2-\alpha_1)} c_{n-1} \quad (4.4.24)$$

We now have an expansion about corner point two in the form of an infinite series of positive powers starting at one with known coefficients. Upon reversion the series will become

$$\frac{1}{\zeta - \xi_1} = \sum_{n=1}^{\infty} a_n \left(Z^{1/(2-\alpha_1)} \right)^n \quad (4.4.25)$$

where the coefficients can be found using the section on series reversion. Note, when evaluating $Z^{1/(2-\alpha_1)}$ in the reversion, the expansion may need to be rotated to go between the branch cuts properly; this is explained in appendix B.

5 SERIES REVERSION

We will find the inverse transformations of the mapping functions $Z(\zeta)$, or $Z(\chi)$, using the reversion of series to obtain the expansions representing $\zeta(Z)$, or $\chi(Z)$. This section will explain the reversion of the far field expansion. The expansions about the two endpoints, and the two corner points will have different coefficients and variables, but are in the same form of a infinite series of positive powers starting at one, so they will follow the same method.

With a series in terms of ψ to represent the mapping function

$$\Xi = \sum_{j=1}^{\infty} b_j \psi^j \quad (5.1)$$

the reversion can be obtained, a series in the form of

$$\psi = \sum_{n=1}^{\infty} c_n \Xi^n \quad (5.2)$$

This is done using the Lagrange inversion formula; it is used for cases like this where $f(\psi) = \Xi$ is known, and $\psi = g(\Xi)$ is to be solved for. f must be analytic at a point a and $f'(a) \neq 0$. g must be analytic at the point $b = f(a)$. The formula is as follows

$$g(\Xi) = a + \sum_{n=1}^{\infty} \left(\lim_{\psi \rightarrow a} \left(\frac{d^{n-1}}{d\psi^{n-1}} \left(\frac{\psi - a}{f(\psi) - b} \right)^n \right) \frac{(\Xi - b)^n}{n!} \right) \quad (5.3)$$

Choosing point $a = 0$, therefore $b = 0$ will work for all of the expansions, as they were written in such a way that this would be possible. Choosing $a = 0$ corresponds to $1/\chi = 0$, $(\zeta - \xi) = 0$, $(\zeta - \xi_1) = 0$ and $1/(\zeta - \xi_1) = 0$ for the far field, endpoints, corner point one and corner point two expansions respectively. The series expansions are analytic at these points, and their derivatives are not

equal to zero. Note, the derivative of the mapping function equals zero at the endpoints; this is not a problem as the expansion about the endpoints were written in terms of a square root. Setting $a = b = 0$ in (5.3) leaves

$$g(\Xi) = \sum_{n=1}^{\infty} \left(\lim_{\psi \rightarrow 0} \left(\frac{d^{n-1}}{d\psi^{n-1}} \left(\frac{\psi}{f(\psi)} \right)^n \right) \frac{\Xi^n}{n!} \right) \quad (5.4)$$

It may be seen that equation (5.4) is in the form of the series in equation (5.2) with the coefficients given as

$$c_n = \frac{1}{n!} \lim_{\psi \rightarrow 0} \frac{d^{n-1}}{d\psi^{n-1}} \left(\frac{\psi}{\sum_{j=1}^{\infty} b_j \psi^j} \right)^n \quad (5.5)$$

We will begin simplifying this expression, first by factoring out ψ

$$c_n = \frac{1}{n!} \lim_{\psi \rightarrow 0} \frac{d^{n-1}}{d\psi^{n-1}} \left(\frac{1}{\sum_{j=1}^{\infty} b_j \psi^{j-1}} \right)^n \quad (5.6)$$

and renaming the coefficients $u_j = b_{j+1}$

$$c_n = \frac{1}{n!} \lim_{\psi \rightarrow 0} \frac{d^{n-1}}{d\psi^{n-1}} \left(\frac{1}{\sum_{j=0}^{\infty} u_j \psi^j} \right)^n \quad (5.7)$$

In order to make taking the $(n-1)^{th}$ derivative of the reciprocal of a series raised to the n^{th} power simpler, first the series within the parenthesis can be written as a new series using the division of series, Knuth (1998).

$$\frac{1}{\sum_{j=0}^{\infty} u_j \psi^j} = \sum_{j=0}^{\infty} w_j \psi^j \quad (5.8)$$

Taking the numerator as a series with the constant equal to one and all other

coefficients equal to zero. The new coefficients can be obtained

$$w_0 = \frac{1}{u_0} \quad (5.9)$$

and for all $j > 0$

$$w_j = \frac{\sum_{k=0}^{j-1} w_k u_{j-k}}{-u_0} \quad (5.10)$$

After substituting equation (5.8) into (5.7) we now have

$$c_n = \frac{1}{n!} \lim_{\psi \rightarrow 0} \frac{d^{n-1}}{d\psi^{n-1}} \left(\sum_{j=0}^{\infty} w_j \psi^j \right)^n \quad (5.11)$$

For each c_n to be solved for, the series within the parenthesis will be raised to the corresponding power. A power series raised to a power can be written as a new series, Knuth (1998).

$$\left(\sum_{n=0}^{\infty} w_n \psi^n \right)^n = \sum_{n=0}^{\infty} v_n \psi^n \quad (5.12)$$

Where the constant is the old constant raised to the n^{th} power

$$v_0 = w_0^n \quad (5.13)$$

and the rest of the coefficients are found using the following formula

$$v_j = \frac{1}{j w_0} \sum_{k=1}^j (kn - j + k) w_k v_{j-k} \quad j = 1, 2, \dots \quad (5.14)$$

Note that there will be a different set of v_j coefficients, for $j \geq 0$, for each c_n to be solved for.

Because the limit is as ψ goes to zero, all of the terms in the derivatives of the series will be zero except for the first, which will be multiplied by a factorial of the order of the derivative

$$\lim_{\psi \rightarrow 0} \frac{d^{n-1}}{d\psi^{n-1}} \sum_{j=0}^{\infty} v_j \psi^j = (n-1)!v_{n-1} \quad (5.15)$$

and the coefficients take the following form.

$$c_n = \frac{1}{n!} (n-1)!v_{n-1} \quad (5.16)$$

6 ANALYTIC CONTINUATION

We now have the reversions of the expansions for the far field, endpoints, and corner points. This will allow us to compute the value of z given the value of χ in the five areas of the domain that have been expanded about. This still leaves some areas of the domain that there is not an inverse mapping for. There is a ring around the two legged slot centered at z_0 with width of $R_1 - R_2$ that is not entirely covered by the endpoint expansions. In order to have the inverse mapping throughout the entire domain, we will use analytic continuation to increase the domain of the far field reversion into the areas surrounding the element where the other expansions are not valid. Figure 6.1 is a diagram showing the shaded areas that will need to be continued into.

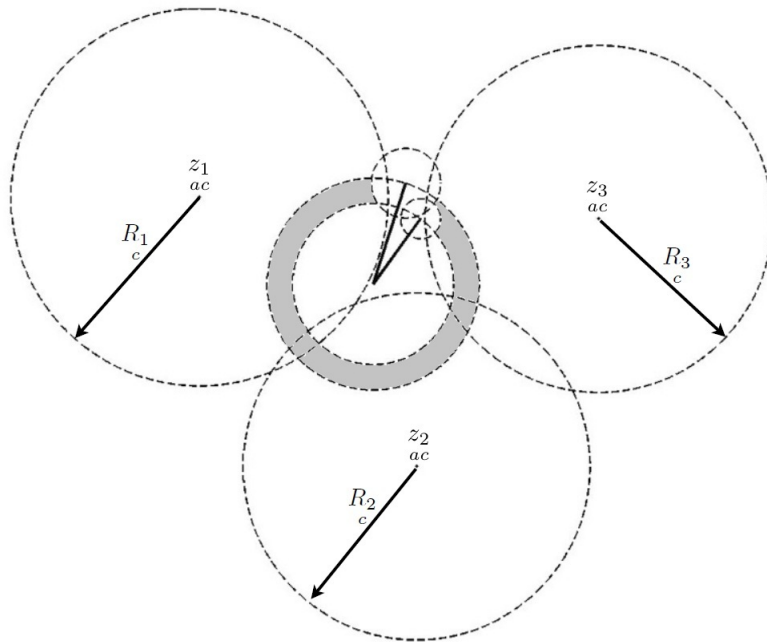


Figure 6.1: The two legged slot in the z plane, along with domains for each expansion. The shaded area is to be continued into.

In general, the area surrounding a two-legged slot will require three analytic continuations of the far field reversion in order to cover the rest of the domain the expansions about the endpoints and corner points did not. The point at which the continuations are chosen to be expanded about in the z plane are labelled z_j _{ac} for $j = 1, 2, 3$. The radius R_j _c chosen for each expansion will vary based on the selected shape and may be different for each expansion. The maximum radius that the analytic continuation expansions will be valid is the shortest distance from the point being expanded about to a singularity or branch cut, which are at the endpoints, corner points and along the two-legged slot.

The analytic continuations of the far field reversion will take the the following form, Churchill (1960).

$$f(Z) = \sum_{n=0}^{\infty} \frac{f^{(n)}\left(\frac{Z}{ac}\right)}{n!} \left(Z - \frac{Z}{ac}\right)^n \quad (6.1)$$

which can also be written as

$$\psi = \sum_{n=0}^{\infty} d_n \left(Z - \frac{Z}{ac}\right)^n \quad (6.2)$$

where $\psi = 1/\chi$ and the coefficients d_n for $n \geq 0$ are

$$d_n = \frac{1}{n!} \frac{d^n}{dZ^n} \sum_{j=1}^{\infty} c_j \frac{Z^{-j}}{ac} \quad (6.3)$$

or

$$d_n = \frac{1}{n!} \sum_{j=1}^{\infty} (-1)^n \frac{(n+j-1)!}{(j-1)!} c_j \frac{Z^{-j-n}}{ac} \quad (6.4)$$

Note that the coefficients c_j are those for the far field reversion, and Z is raised to negative powers because the expansion was in the form of $1/Z$. Replacing Z _{ac} in the equations above with the expansion points Z_1 _{ac}, Z_2 _{ac} and Z_3 _{ac}, will give a different set of coefficients for each expansion.

7 THE FUNCTIONS $\chi(z)$

For any point z we can now find the corresponding value of χ . However, we need a procedure for determining which expansion to use for each point z through out the domain. The entire domain will be divided into eight subsections, one for the far field, two for the corner points, two for the end points, and three for the analytic continuations. With the exception of the far field, each subsection will be created in such a way that its domain has a radius has unit length. This can be viewed as a transformation similar to the transformation from z to Z .

$$Z = \frac{z - z_0}{R_1} \quad (7.1)$$

Some of the domains will overlap and a choice will have to be made on which expansion to use in the area of their union. In general, every thing in the far field will use the far field expansion, not the expansion about the endpoints or the analytic continuation. Also, it is chosen that the area within the radius of the shorter leg will use the corner point expansions, not the endpoints or analytic continuation. Within the ring between the short and long leg, it is chosen to use the expansion about the end points first, then cover any left over area with analytic continuation. The choices are based upon ease of evaluation.

Far Field

The far field reversion will be used every where out side of the unit circle in the Z plane. Where

$$Z\bar{Z} \geq 1 \quad (7.2)$$

the corresponding value for χ can be calculated.

$$\chi = \left[\sum_{n=1}^{\infty} c_n \left(\frac{1}{Z} \right)^n \right]^{-1} \quad (7.3)$$

Corner Points

The domain for the corner point expansions will be in a circle centered at the corner points with radius of the shorter leg. A new complex variable is defined to assist in defining the corner points domain.

$$D_{cp} = \frac{ZR_1}{R_2} \quad (7.4)$$

Two additional parameters will be used in separating the domain for the corner points, the slope of each leg.

$$m_1 = \frac{\Im Z_1}{\Re Z_1} \quad m_2 = \frac{\Im Z_2}{\Re Z_2} \quad (7.5)$$

Now, if the point that is being evaluated lies within the corner points domain

$$D_{cp} \bar{D}_{cp} \leq 1 \quad (7.6)$$

we must determine which side of the slot the point lies. The following steps are an example that corresponds with figure 6.1. Because identical slots can be made, the domain for corner points one and two may be switched. If the following conditions are met

$$\Re Z \leq \frac{\Im Z}{m_1} \quad \Re Z \geq \frac{\Im Z}{m_2} \quad (7.7)$$

the point is in the domain of corner point two, and the value for ζ can be calculated. When evaluating the expansion the branch cut must be accounted for. The values θ_{cp} are the amount the expansions may need to be rotated as explained in appendix B.

$$\zeta = \left[\sum_{n=1}^{\infty} a_n \left(e^{\frac{i\theta_2}{cp}(2-\alpha_1)} \left(Z e^{-\frac{i\theta_2}{cp}} \right)^{1/(2-\alpha_1)} \right)^n \right]^{-1} + \xi_1 \quad (7.8)$$

If the conditions in (7.7) are not met, the point is in the domain of corner point one, and the value for ζ can be calculated

$$\zeta = \sum_{n=1}^{\infty} a_n \left(e^{\frac{i\theta_1}{cp\alpha_1}} \left(Z e^{-\frac{i\theta_1}{cp}} \right)^{1/\alpha_1} \right)^n + \xi_1 \quad (7.9)$$

with ζ known, the corresponding value of χ may be found.

$$\chi = \left(\frac{2}{\zeta - i} - i \right) \nu \quad (7.10)$$

End Points

The reversions of the expansions about the end points will be used inside of the domain of the far field, and outside the domain of the corner points

$$Z\bar{Z} \leq 1 \quad D\bar{D}_{cp} \geq 1 \quad (7.11)$$

Two new dimensionless complex variables will be used to assist in defining the domain for each end point.

$$D_1 = \frac{z - z_1}{R_1 \epsilon_1} \quad D_2 = \frac{z - z_2}{R_2 \epsilon_2} \quad (7.12)$$

If the following condition is met for the point being evaluated along with the conditions in (7.11) the point will lie in the domain of end point one

$$D_1 \overline{D_1} \leq 1 \quad (7.13)$$

and ζ can be calculated. When evaluating the expansion the branch cut must be accounted for, and rotated if necessary, the values θ_{ep} are the amount the branch cuts may need to be rotated as explained in appendix B.

$$\zeta = \sum_{n=1}^{\infty} a_n \left(e^{\frac{i\theta_1}{2}} \sqrt{\left(Z - Z_1 \right) e^{-\frac{i\theta_1}{ep}}} \right)^n + \xi_{1ep} \quad (7.14)$$

If the following condition is met for the point being evaluated, along with the conditions in (7.11), the point will lie in the domain of end point two.

$$D_2 \overline{D_2} \leq 1 \quad (7.15)$$

ζ can be calculated

$$\zeta = \sum_{n=1}^{\infty} a_n \left(e^{\frac{i\theta_2}{2}} \sqrt{\left(Z - Z_2 \right) e^{-\frac{i\theta_2}{ep}}} \right)^n + \xi_{2ep} \quad (7.16)$$

with ζ known, the corresponding value of χ may be found.

$$\chi = \left(\frac{2}{\zeta - i} - i \right) \nu \quad (7.17)$$

If the point happens to lie in the union of the domains for each endpoint, either expansion may be used.

Analytic Continuation

The analytic continuation expansions will be used to cover what is left of

the domain. There will be three continuations of the far field reversion. The three expansions will overlap; where they do, either expansion may be used. Analytic continuation will be used inside of the domain of the far field, outside the domain of the corner points, and outside the domain of the end points. Where

$$Z\bar{Z} \leq 1 \quad \underset{cp\ cp}{D\bar{D}} \geq 1 \quad \underset{ep\ ep}{D_1\bar{D}_1} \geq 1 \quad \underset{ep\ ep}{D_2\bar{D}_2} \geq 1 \quad (7.18)$$

Three new dimensionless complex variables will be defined to assist in defining the domain for each analytic continuation of the far field reversion.

$$D_1 = \frac{z - z_1}{\underset{c}{R_1} \underset{ac}{ac}} \quad D_2 = \frac{z - z_2}{\underset{c}{R_2} \underset{ac}{ac}} \quad D_3 = \frac{z - z_3}{\underset{c}{R_3} \underset{ac}{ac}} \quad (7.19)$$

If the following condition is met for the point being evaluated along with the conditions in (7.18) the point will lie in the domain of the first analytic continuation

$$\underset{ac}{D_1} \underset{ac}{\bar{D}_1} \leq 1 \quad (7.20)$$

and the corresponding value for χ can be calculated.

$$\chi = \left[\sum_{n=0}^{\infty} \underset{ac1}{d_n} \left(\underset{ac}{Z} - \underset{ac}{Z_1} \right)^n \right]^{-1} \quad (7.21)$$

If the following condition is met for the point being evaluated along with the conditions in (7.18) the point will lie in the domain of the second analytic continuation

$$\underset{ac}{D_2} \underset{ac}{\bar{D}_2} \leq 1 \quad (7.22)$$

and the corresponding value for χ can be calculated.

$$\chi = \left[\sum_{n=0}^{\infty} \frac{d_n}{ac^2} \left(Z - \frac{Z_2}{ac} \right)^n \right]^{-1} \quad (7.23)$$

If the following condition is met for the point being evaluated along with the conditions in (7.18) the point will lie in the domain of the third analytic continuation

$$\frac{D_3 \overline{D_3}}{ac \ ac} \leq 1 \quad (7.24)$$

and the corresponding value for χ can be calculated.

$$\chi = \left[\sum_{n=0}^{\infty} \frac{d_n}{ac^3} \left(Z - \frac{Z_3}{ac} \right)^n \right]^{-1} \quad (7.25)$$

With a method for evaluating the various functions $\chi(z)$ we can now create solutions using analytic elements.

8 ANALYTIC ELEMENTS

In this section we will discuss solutions for an arbitrary number of analytic elements of arbitrary shape. The method used is very similar to that of cylindrical elements, as they are both mapped onto the unit circle, and will closely follow the solution for cylindrical analytic elements, Strack (2012). First, we will discuss the solution for lakes. We consider the case of flow with multiple arbitrary shaped equipotentials and other elements such as uniform flow and wells. The head is known at a reference point z_r , and the corresponding value for the discharge potential is Φ_r .

The analytic element method will be used to superimpose analytic functions that will satisfy the boundary conditions. Each element will be based on its own two-legged slot, with corner point z_m , leg with longer length R_{1m} , and its own local coordinate system

$$Z_m = \frac{z - z_m}{R_{1m}} \quad (8.1)$$

as well as its own upper half plane, and χ plane.

$$\zeta_m = \zeta(Z_m) \quad \chi_m = \chi(Z_m) \quad (8.2)$$

First, we will construct an analytic element for an arbitrary shaped lake. The complex potential for this element is holomorphic outside of the unit circle in the χ plane, and thus can be represented with its asymptotic expansion. We write the complex potential Ω_m as the asymptotic expansion in terms of χ_m plus a logarithmic term that represents the net flow into the lake, Q_m . The complex potential for the m^{th} element is

$$\Omega_m = \sum_{n=1}^{\infty} \alpha_n \chi_m^{-n} + \frac{Q}{2\pi} \ln \left| \frac{\chi_m}{\chi_r} \right| \quad (8.3)$$

Note that the term representing the flow into the lake was written such that it has no contribution to the potential at χ_r , the point in the elements χ plane that corresponds to the reference point z_r . This is chosen because the effect of the logarithmic term grows with distance, while the effect of the sum decreases. This will improve the convergence process of solving for the unknowns.

We construct the solution for M of these elements by adding the effect of given elements, Ω_g that may represent wells and uniform flow, M complex potentials in the form of (8.3), and a constant C .

$$\Omega = \Omega_g + \sum_{m=1}^M \Omega_m(\chi) + C \quad (8.4)$$

We choose the function Ω_g for now as the complex potential for uniform flow, i.e.,

$$\Omega_g = -Wz \quad (8.5)$$

where W_0 is a complex discharge vector, defined as

$$W_0 = Q e^{-i\alpha} \quad (8.6)$$

Q_0 is the magnitude of the discharge vector and α is the angle between the discharge vector and the x axis. We require that the elements do not intersect each other and determine the coefficients α_n in such a way that the walls of the shapes are equipotentials, $\Re\Omega = \Phi$ is constant along each the boundary of each shape.

An iterative procedure is used to solve for the coefficients in the complex

potential for one analytic element at a time, treating the coefficients in the complex potentials for all the other elements as known. The complex potential for any of the analytic elements is holomorphic outside the boundary associated with that element, and is not holomorphic inside the boundary associated with the analytic element whose unknowns we are solving for, due to the singularities on the corner points and endpoints of the two-legged slot. We will use the real part of the complex potential, the discharge potential, which is constant inside the boundary of the element, to expand the complex potential in a Taylor series about the center of the circle that corresponds to that element in its χ plane. We will see that this expansion allows us to solve for the unknown coefficients in the expansion (8.3) that represents element j everywhere outside its boundary. We write the complex potential as the sum of that for element j , Ω_j , plus a function Ω_{other} , which is the sum of the complex potentials for all other elements plus the uniform flow term

$$\Omega = \Omega_j + \Omega_{other} + C \quad (8.7)$$

where Ω_j is given by (8.3), and where

$$\Omega_{other} = \sum_{\substack{m=1 \\ m \neq j}}^M \Omega_m + \Omega_g \quad (8.8)$$

We expand Ω_{other} about the center of the shape in the χ_j plane, in a Taylor series

$$\Omega_{other} = \sum_{n=0}^{\infty} a_n \chi_j^n \quad (8.9)$$

We obtain expressions for the complex constants a_n in the manner of a Fourier

series, using the real part of the complex potential $\Phi = 1/2(\Omega + \bar{\Omega})$

$$a_n = \frac{1}{2\pi} \oint_C \frac{1}{2} \left(\Omega_{other} (z(\chi)) + \overline{\Omega_{other} (z(\chi))} \right) e^{-in\theta} d\theta \quad n = 0, 1, 2, \dots \quad (8.10)$$

where θ is along the unit circle in the χ plane

$$\chi = e^{i\theta} \quad (8.11)$$

Evaluation of the integral (8.10) for different values of n will produce the values of the unknown coefficients a_n in the expansion of Ω_{other} , valid along the boundary of the circular equipotential in the χ plane.

The complex potential for element j is

$$\Omega_j = \sum_{n=1}^{\infty} \alpha_n \chi_j^{-n} + \frac{Q}{2\pi} \ln \left| \frac{\chi_j}{\chi_{rj}} \right| \quad (8.12)$$

The boundary condition along the perimeter of the element is that the potential is constant. The complex potential along the boundary of the element is the sum of Ω_{other} (8.9) and Ω_j (8.12).

$$\Omega = \sum_{n=0}^{\infty} a_n \chi_j^n + \sum_{n=1}^{\infty} \alpha_n \chi_j^{-n} + \frac{Q}{2\pi} \ln \left| \frac{\chi_j}{\chi_{rj}} \right| \quad \chi_j \bar{\chi}_j = 1 \quad (8.13)$$

We use the condition that χ represents a point on the boundary of the element, i.e.,

$$\chi_j^{-n} = \bar{\chi}_j^n \quad (8.14)$$

so that (8.13) becomes

$$\Omega = \sum_{n=0}^{\infty} a_n \chi_j^n + \sum_{n=1}^{\infty} \alpha_n \chi_j^n + \frac{Q}{2\pi} \ln \frac{\chi_j}{\left| \chi_r \right|} \quad \chi_j \bar{\chi}_j = 1 \quad (8.15)$$

The boundary condition is that the potential Φ is constant along the perimeter of the shape; this condition is met if the sum of the first two terms in (8.15) is purely imaginary, i.e., if the coefficients α_n satisfy the following conditions

$$\alpha_n = -\bar{a}_n \quad n > 0 \quad (8.16)$$

We obtain an expression for the potential along the perimeter of the element by taking the real part of (8.15), and setting it equal to the given value of the potential along the boundary, Φ_j

$$\Phi = \Phi_j = \Re a_0 + \frac{Q}{2\pi} \ln \frac{1}{\left| \chi_r \right|} \quad (8.17)$$

We solve for the unknown net flow into the lake, Q and obtain

$$Q = 2\pi \frac{\Phi_j - \Re a_0}{\ln \left[1 / \left| \chi_r \right| \right]} \quad (8.18)$$

We will solve for the coefficients a_n for one element at a time, and use the values of these coefficients to determine the values of α_n . When solving for the coefficients of the next element, the updated coefficients from the previous element are then used in the complex potential Ω_{other} . The process is repeated until the coefficients α_n do not change from the previous iteration beyond a certain chosen value. The constant C may then be solved for after looping over all the cylinders, using the potential at the reference point Φ_r .

An example of five fixed head analytic elements of arbitrary shape repre-

senting lakes in a field of uniform flow can be seen in figure 8.1.

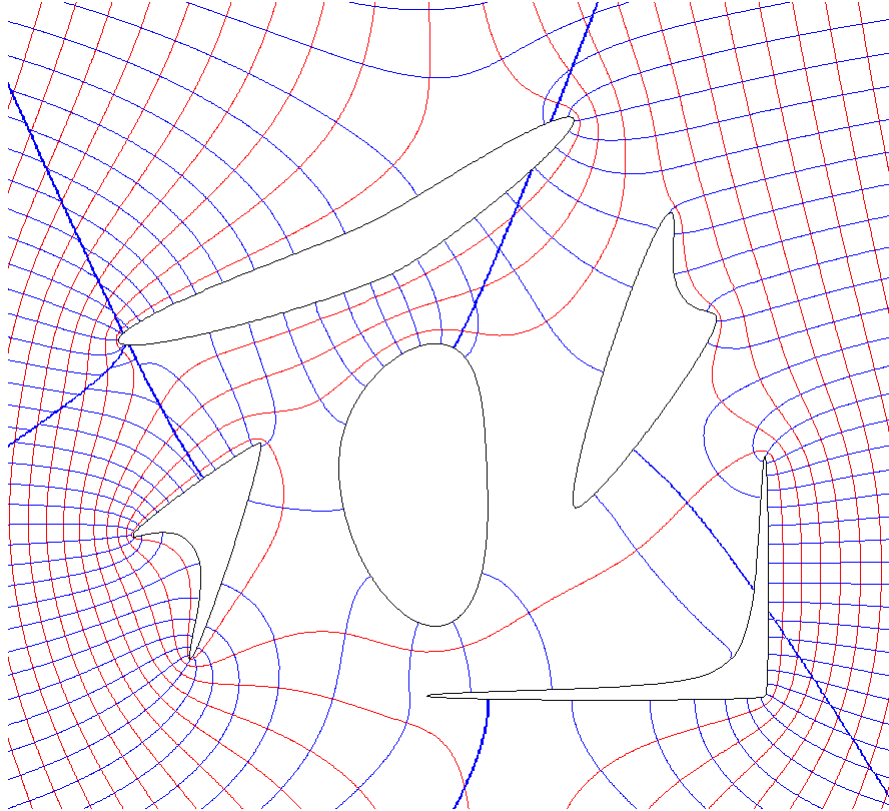


Figure 8.1: Flownet for lakes in a field of uniform flow.

9 ADDITIONAL SHAPES

The analysis for an analytic element of arbitrary shape was carried out for an element based on a two-legged slot, the analysis may be extended to cover a larger extent of shapes. In theory any shape could be made using different mappings, assuming the inverse mappings can be obtained. For the two-legged slot, there were a total of eight series expansions required to obtain the inverse mapping for the entire domain, for more complicated shapes, this number would most likely increase. The mappings from the upper half plane and to the χ plane are where the degrees of freedom in the shape were introduced, by adding degrees of freedom additional shapes can be made. One immediate example, is basing the element on a three-legged slot.

The mapping for a three-legged slot is a piece wise constant transformation for a polygon that contains the origin and not infinity. It is the same as that for the two-legged slot, except the numerator gains a term $(\zeta - \xi_2)^{\alpha_2}$.

$$Z = |A|_r e^{i\alpha_0} \frac{(\zeta - \xi_1)^{\alpha_1} (\zeta - \xi_2)^{\alpha_2}}{(\zeta + i)(\zeta - i)} \quad (9.1)$$

Where α_2 is the angle between the legs at the additional corner point ξ_2 . The values ξ_1 and ξ_2 are to be determined by the ratio of the lengths of the legs. The transformation from the upper half plane onto the three-legged slot is shown in figure 9.1.

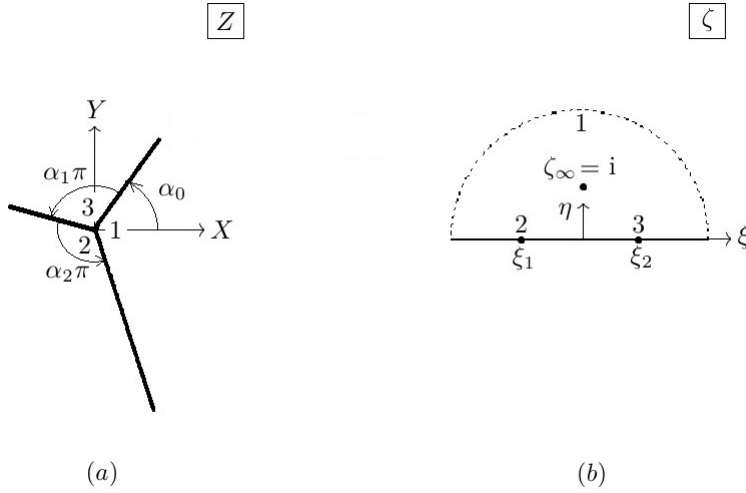


Figure 9.1: The slot in the Z plane (a) and the upper half plane ζ (b).

The rest of the mappings between z and Z and between ζ and χ will remain the same as those used for the two-legged slot. The far field expansion and reversion will remain approximately the same, as well as the process for analytic continuation. The expansions about the endpoints and corner points would be slightly different, and all of the algebra and series expansion manipulations would need to be carried out again. Neglecting the expansions about the corner points and endpoints, some single sided elements can still be made. Single sided elements, such as lakes and impermeable objects do not require an expansion inside of the boundary of the element, as the condition is fixed by definition. Using the far field expansion and reversion along with analytic continuation will cover enough of the domain that some shapes will still be able to be used. An example solution for a lake and an impermeable object will be demonstrated.

The complex potential for a lake in a field of uniform flow with a well, Strack (1989).

$$\Omega = Q_u^* e^{-i\gamma} \left(\chi - \frac{1}{\chi} \right) + \frac{Q}{2\pi} \ln \left[\frac{\chi - \chi_w}{\chi - 1/\bar{\chi}_w} \frac{1}{|\chi_w|} \right] \quad (9.2)$$

where Q_u^* represents the discharge of the uniform flow in the χ plane and γ its orientation there, Q is the discharge of the well χ plane and χ_w its location there. An example of an element constructed using a three-legged slot representing a lake in a field of uniform flow with a well is shown in figure 9.2. Note, in this example $Q \gg Q_u^*$.

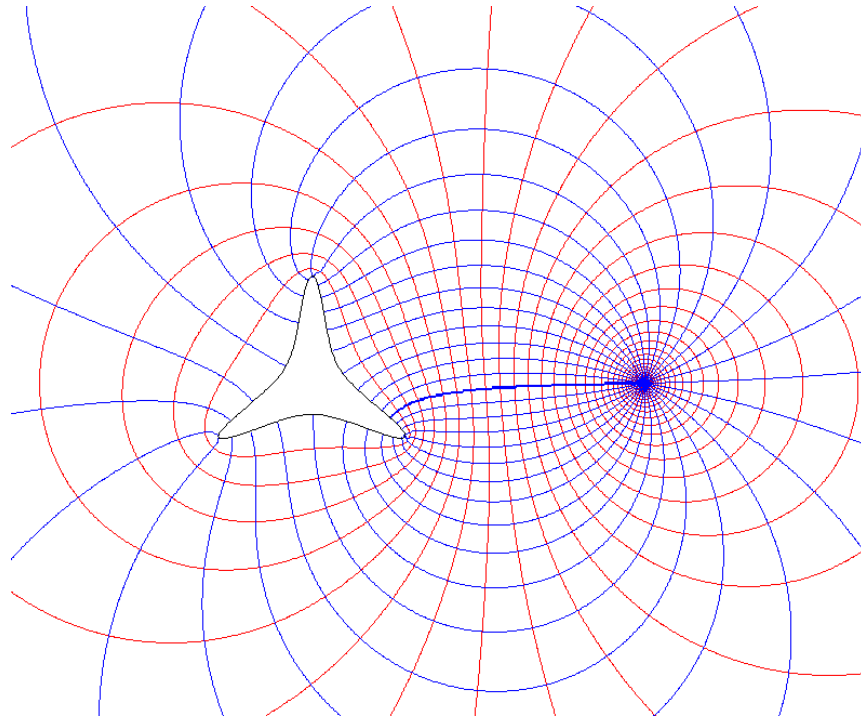


Figure 9.2: Flownet for a lake and a well in a field of uniform flow.

The complex potential for an impermeable object in a field of uniform flow with a well, Strack (1989).

$$\Omega = Q_u^* e^{-i\gamma} \left(\chi + \frac{1}{\chi} \right) + \frac{Q}{2\pi} \ln \left[\frac{(\chi - \chi_w)(\chi - 1/\bar{\chi}_w)\bar{\chi}_w}{-\chi} \right] \quad (9.3)$$

An example of an element constructed using a three-legged slot representing an impermeable object in a field of uniform flow with a well is shown in figure 9.3.

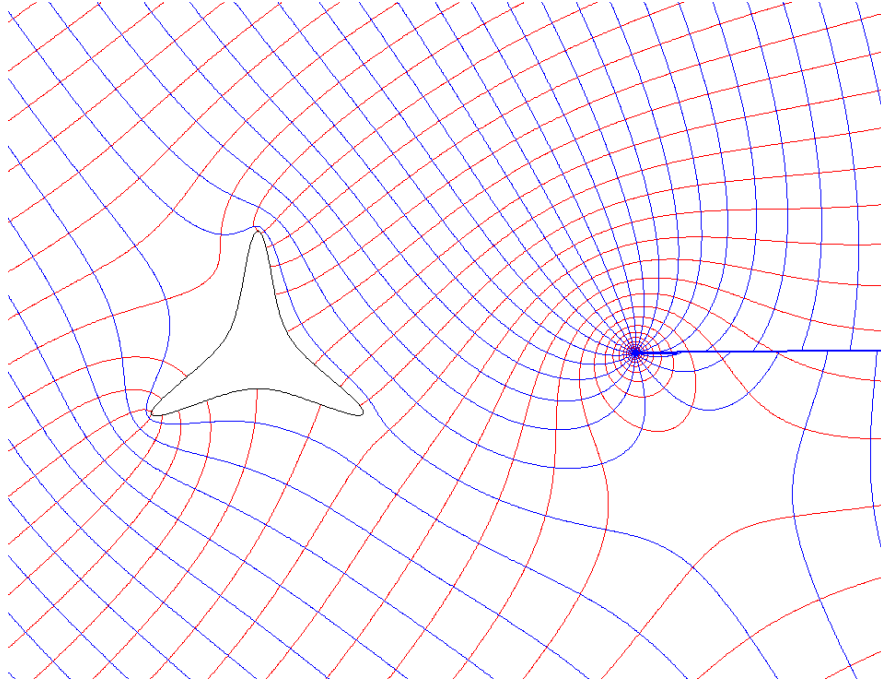


Figure 9.3: Flownet for an impermeable object and a well in a field of uniform flow.

More degrees of freedom may be added. For the case of N legs the mapping function gains a term in the numerator for each additional leg, and $Z = Z(\zeta)$ becomes

$$Z = \frac{|A| e^{i\alpha_0} \prod_{n=1}^{N-1} (\zeta - \xi_n)^{\alpha_n}}{(\zeta + i)(\zeta - i)} \quad (9.4)$$

Additional degrees of freedom could be introduced in the mapping from the upper half plane onto the unit circle in the χ plane. The analogous complex potential used in creating an equipotential around the two-legged slot could be modified. The analogous complex potential consisted of a recharge well in the upper half plane and an image well in the lower half plane. By adding additional elements to the analogous complex potential the equipotential around the slot could be changed dramatically.

$$\Omega_{map} = \frac{Q}{2\pi} \ln \frac{\zeta + i}{\zeta - i} + \Omega_{other} \quad (9.5)$$

For example, an additional well and image well could be added to the analogous complex potential, causing the once circular equipotentials in the upper half plane to become stretched or pushed in the direction of the well, this would result in a corresponding distortion of the equipotential around the slot in the z plane. The transformation from ζ to χ would then need to be rewritten to include the new parameters associated with the additional degrees of freedom. Another variation could be to base the elements shape off of something other than a multi-legged slot.

10 REFERENCES

Barnes R., Janković I. High order line elements in modeling two-dimensional groundwater flow. *Journal of Hydrology*, 211-223, 1999.

Barnes R., Janković I. Two-dimensional flow through large numbers of circular inhomogeneities. *Journal of Hydrology*, 226:204-210, 1999.

Churchill, Ruel V. *Complex Variables and Applications*. 2nd ed. New York: McGraw-Hill, 1960.

Edlund, Micheal D. *A Conformal Mapping Application to the Analytic Element Method*. M.S. Thesis. Department of Civil Engineering, University of Minnesota - Minneapolis. 1991.

"Minneapolis, Minnesota." Map. Google Maps. Google, 4 November 2012. Web. 4 November 2012.

Knuth, Donald. *Seminumerical Algorithms*. 3rd ed. Berkeley: Addison Wesley Longman, 1998.

Olver, Peter J. *Introduction to Partial Differential Equations*. Draft. 2012.

Salisbury, Melinda L. *Control Equation Formulation for Circular Inhomogeneities in the Analytic Element Method*. M.S. Thesis. Department of Civil Engineering, University of Minnesota - Minneapolis. 1992.

Strack, Otto D.L., Haitjema, H. M. Modeling double aquifer flow using a comprehensive potential and distributed singularities, 1 , Solution for homogeneous permeabilities. *Water Resour. Res.*, 17(5), pp. 1535-1549. 1981(a).

Strack, Otto D.L., Haitjema, H. M. Modeling double aquifer flow using a comprehensive potential and distributed singularities, 2 , Solution for homogeneous permeabilities. *Water Resour. Res.*, 17(5), pp. 1551-1560. 1981(b).

Strack, Otto D.L. *Groundwater Mechannics*. North Oaks: Strack Consulting, Inc. 1989.

Strack, Otto D.L. *Applied Groundwater Mechannics*. Draft. 2012.

Suribhadla R., Bakker M., Bandilla K., Janković I. Steady two-dimensional groundwater flow through many elliptical inhomogeneities. *Water Resources Research*, 40 (W04202):1-10, 2004.

A VARIOUS SHAPES

Table A.1: Two legged slots with contours of $\nu = 0.5, 0.7, 0.9$ using various values of ξ_1 and α_1 with $\alpha_0 = 0$ and $|A|_r = 1$.

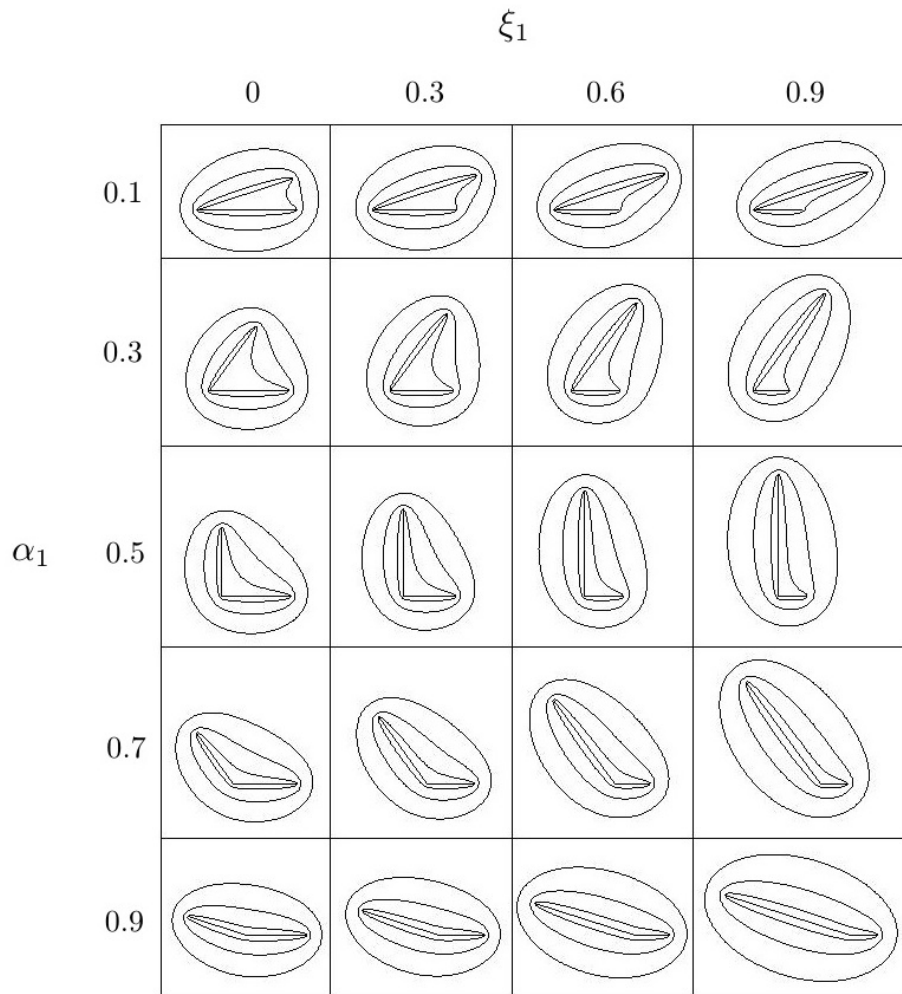
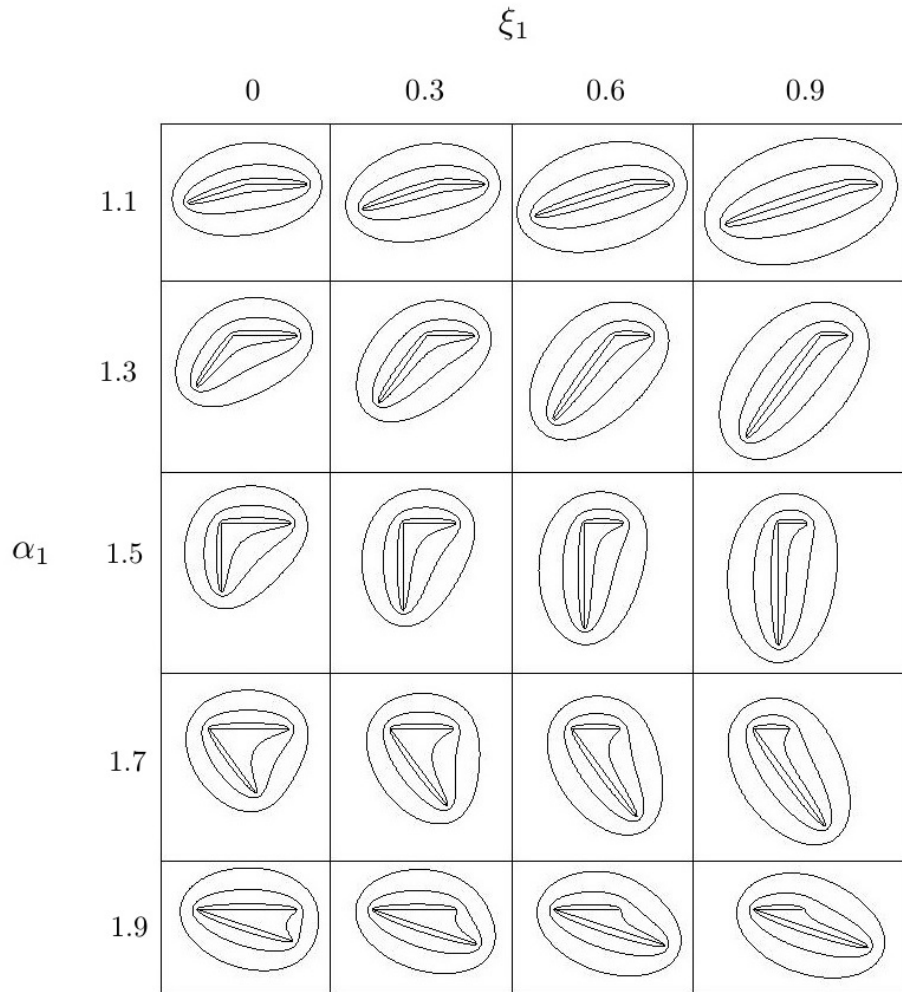


Table A.2: Two legged slots with contours of $\nu = 0.5, 0.7, 0.9$ using various values of ξ_1 and α_1 with $\alpha_0 = 0$ and $|\frac{A}{r}| = 1$.



Tables A.3 and A.4 contain shapes made using negative values of ξ_1 , this interchanges the the lengths of the legs. These shapes replicate those made using positive values of ξ_1 but are at a different orientation. Identical shapes can be made by switching the sign of the value for ξ_1 , changing the value of α_1

to $(2 - \alpha_1)$, and reorienting the shape. Figure A.1. shows a slot identical to the slot shown in figure 2.2 made with different parameters.

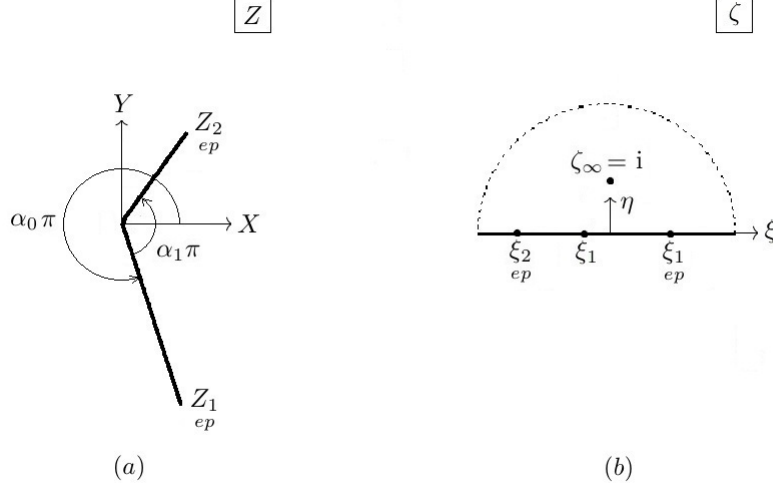


Figure A.1: The slot in the Z plane (a) and the upper half plane ζ (b).

When switching the parameters to create the identical slot, the endpoints in the Z plane will remain the same, as they are labelled according to which leg is longer. The end points in the upper half plane will change because the ratio of the lengths between ξ_1 and the endpoints in the upper half plane has changed. The boundary conditions are then slightly modified for this case.

Alternate Boundary Conditions of the Function $Z(\zeta)$

$$\eta = 0 \quad -\infty < \xi < \xi_{2_{ep}} \quad Z = |Z|e^{i(\alpha_0 + \alpha_1)\pi} \quad 0 < |Z| < |Z_{2_{ep}}| \quad (\text{A.1})$$

$$\eta = 0 \quad \xi_{2_{ep}} < \xi < \xi_1 \quad Z = |Z|e^{i(\alpha_0 + \alpha_1)\pi} \quad |Z_{2_{ep}}| < |Z| < 0 \quad (\text{A.2})$$

$$\eta = 0 \quad \xi_1 < \xi < \xi_{1_{ep}} \quad Z = |Z|e^{i\alpha_0\pi} \quad 0 < |Z| < |Z_{1_{ep}}| \quad (\text{A.3})$$

$$\eta = 0 \quad \xi_{1_{ep}} < \xi < \infty \quad Z = |Z|e^{i\alpha_0\pi} \quad |Z_{1_{ep}}| < |Z| < 0 \quad (\text{A.4})$$

Table A.3: Two legged slots with contours of $\nu = 0.5, 0.7, 0.9$ using various values of ξ_1 and α_1 with $\alpha_0 = 0$ and $|A_r| = 1$.

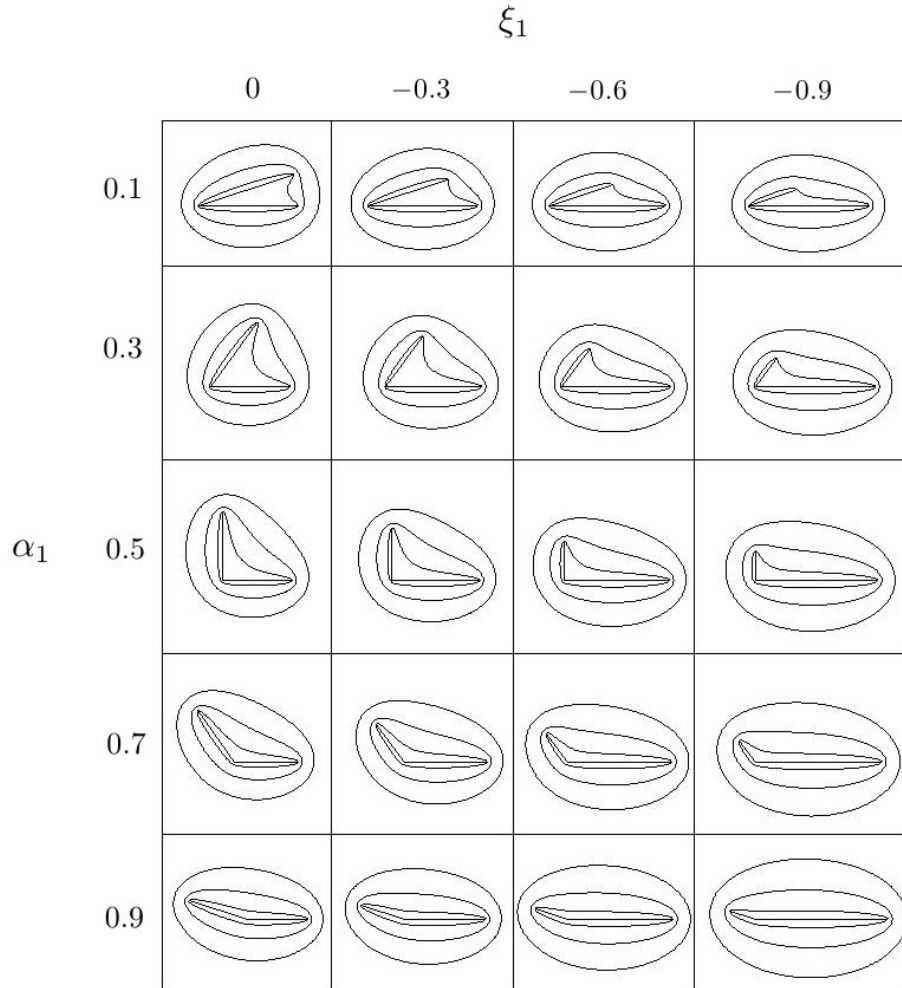
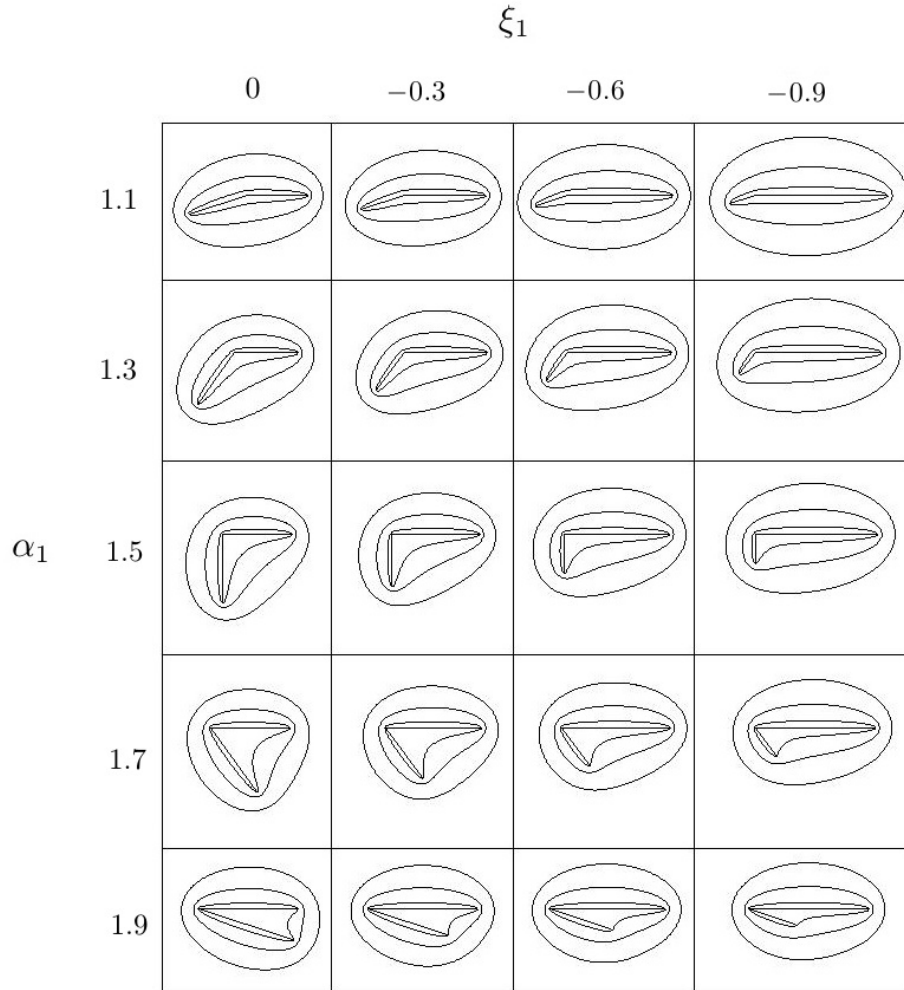


Table A.4: Two legged slots with contours of $\nu = 0.5, 0.7, 0.9$ using various values of ξ_1 and α_1 with $\alpha_0 = 0$ and $|\frac{A}{r}| = 1$.



B BRANCH CUTS

The reversions of the series expansions about the endpoints have Z raised to the one half power, therefore there will be branch cuts emanating from the point being expanded about. Depending upon the geometry and orientation of the two-legged slot, the branch cuts may need to be rotated. The following steps are assuming that when evaluating the reversion of the series expansions the default branch cut is parallel to the real axis of the Z plane in the negative direction, parallel to the $-X$ axis. The branch cut from each end point will need to be rotated to go along the corresponding leg. The exception is when the leg lies along the $+X$ axis, when the branch cut is as it should be. The branch cuts change direction at the corner points, and the orientation of the corner point expansions may need to be adjusted as well. An example of the amount each branch cut will need to be rotated can be seen in figure B.1.

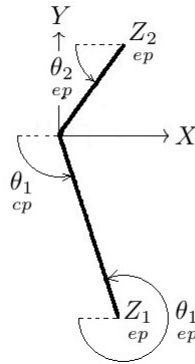


Figure B.1: The amount the branch cuts need to be rotated about the endpoints and the adjustment for a corner point.

The square root in the reversion of the expansion about the end points,

equation (4.2.26), will need to be modified as follows in order to rotate the branch cut to the desired position. Where θ is replaced with θ_1 for the expansion about Z_1 , and θ_2 for the expansion about Z_2 .

$$\sqrt{Z - Z_{ep}} = e^{i\theta/2} \sqrt{\left(Z - Z_{ep}\right) e^{-i\theta}} \quad (\text{B.1})$$

The α_1^{th} root in the reversion of the expansion about corner point one, equation (4.3.14), will need to be modified as follows in order to rotate the expansion to the desired position.

$$Z^{1/\alpha_1} = e^{i\theta_1/\alpha_1} \left(Z e^{-i\theta_1/c_p} \right)^{1/\alpha_1} \quad (\text{B.2})$$

The $(2 - \alpha_1)^{th}$ root in the reversion of the expansion about corner point two, equation (4.4.25), will need to be modified as follows in order to rotate the expansion to the desired position.

$$Z^{1/(2-\alpha_1)} = e^{i\theta_2/(2-\alpha_1)} \left(Z e^{-i\theta_2/c_p} \right)^{1/(2-\alpha_1)} \quad (\text{B.3})$$

Note, the θ values for each expansion will be zero if the branch cuts do not need to be rotated.

C THE ANALOGOUS COMPLEX POTENTIAL

The following flow nets are those of the analogous complex potential that was used in creating the equipotential around the two-legged slot that was used as the boundary for the element. The desired equipotential chosen as the boundary for the element is emphasized with a bold outline. In the z and Z planes the analogous complex potential is that of flow from infinity towards the slot.

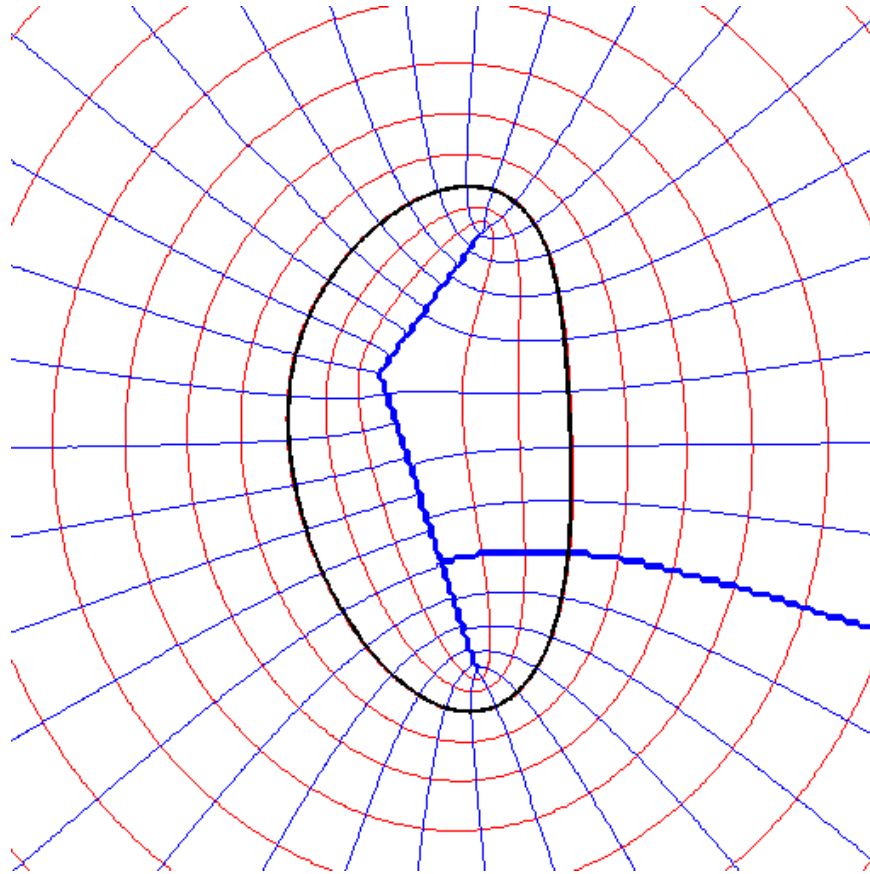


Figure C.1: The analogous complex potential in the Z plane.

Flow from infinity toward the slot in the z plane corresponds to flow from a recharge well at $\zeta = i$ to an image well at $\zeta = -i$. The lower half plane has a shaded back ground.

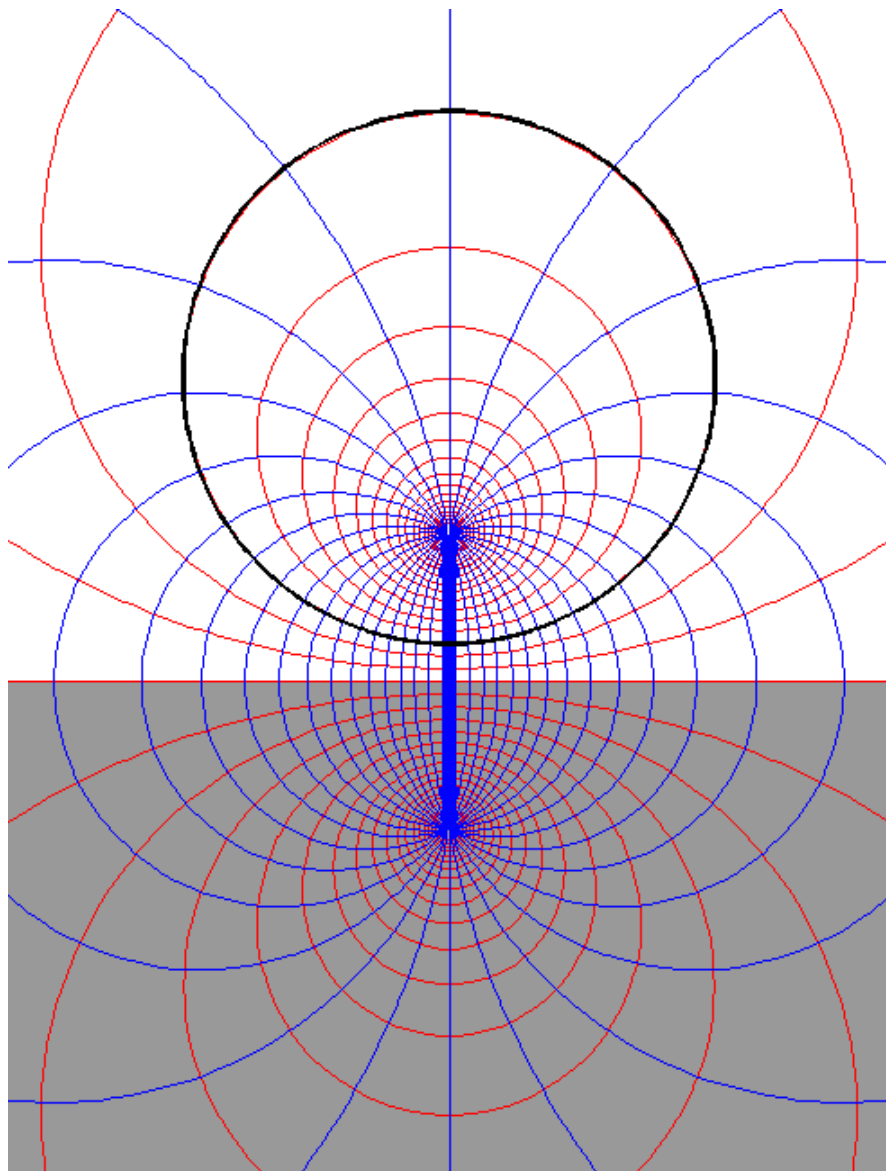


Figure C.2: The analogous complex potential in the ζ plane.

Flow from infinity toward the slot in the z plane corresponds to flow from infinity to a point sink at the origin in the χ plane. The lower half plane (shaded) maps to the interior of the unit circle (shaded).

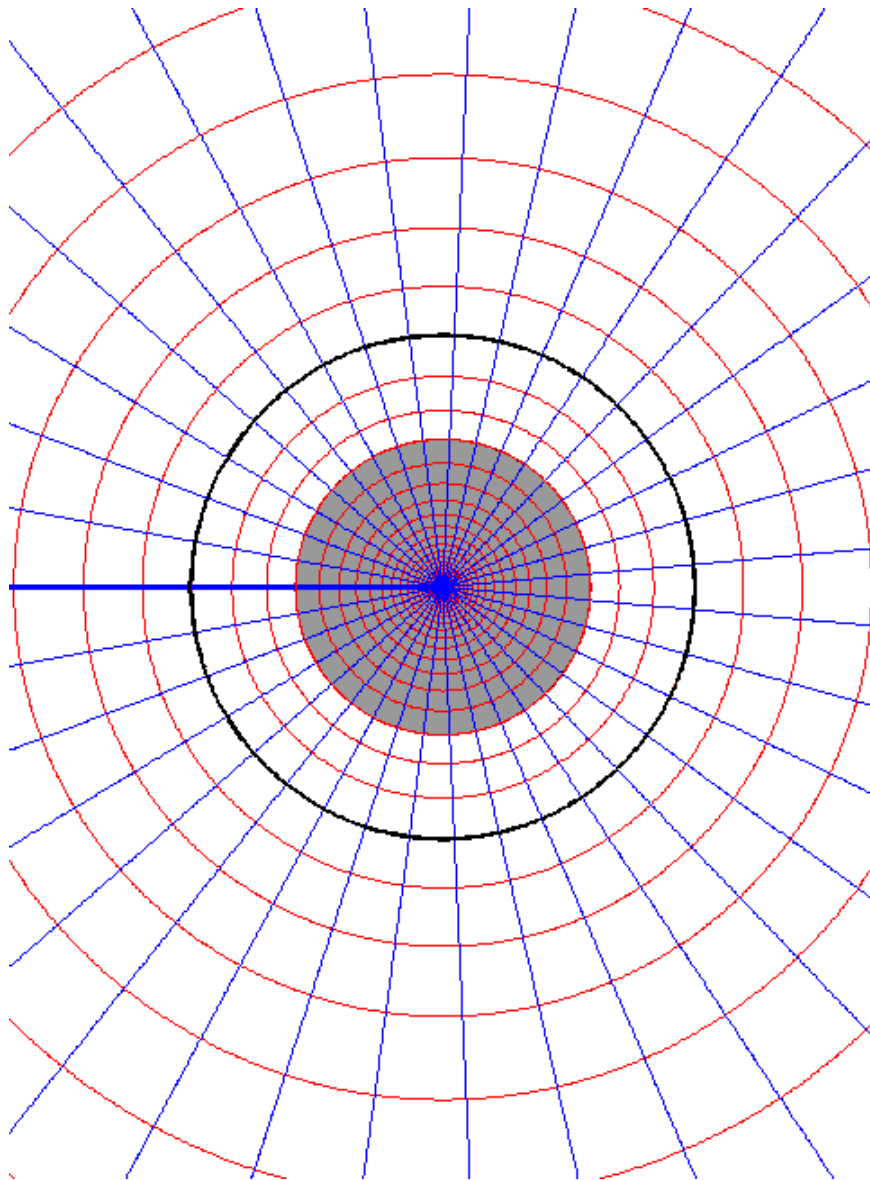


Figure C.3: The analogous complex potential in the χ plane.